

Robust isogeometric preconditioners for the Stokes system based on the Fast Diagonalization method ^{*}

M. Montardini [†] G. Sangalli^{†‡} M. Tani [†]

September 17, 2018

Abstract

In this paper we propose a new class of preconditioners for the isogeometric discretization of the Stokes system. Their application involves the solution of a Sylvester-like equation, which can be done efficiently thanks to the Fast Diagonalization method. These preconditioners are robust with respect to both the spline degree and mesh size. By incorporating information on the geometry parametrization and equation coefficients, we maintain efficiency on non-trivial computational domains and for variable kinematic viscosity. In our numerical tests we compare to a standard approach, showing that the overall iterative solver based on our preconditioners is significantly faster.

Keywords: Isogeometric analysis, k -method, preconditioning, Stokes system, tensor product, Kronecker product.

1 Introduction

Isogeometric analysis (IGA) has been introduced by T.J.R. Hughes et al. in the seminal paper [1]. IGA is an innovative numerical method to discretize partial differential equations (PDEs), based on using the same functions that describe the computational domain in computer-aided design (CAD) systems also for the representation of the solution. These functions are B-Splines or NURBS or generalizations of them. For a complete description of the method and an overview of various engineering applications, see [2]. For a mathematical-oriented overview of IGA we refer to [3].

IGA is a high-order numerical method, when high-degree polynomial/spline approximation is adopted. However within IGA there is the possibility of high-regularity approximating functions. The typical case is indeed when splines of degree p and global C^{p-1} regularity are used within each patch. This is called the isogeometric k -method, which presents significant advantages in comparison to C^0 finite elements of degree p , from many points of view: higher accuracy per degree-of-freedom (see [4, 3]), improved spectral behaviour (see [5]), the possibility of dealing directly with higher-order PDEs ([6] is the first paper in this direction) or constructing smooth structure-preserving schemes (see [7]).

^{*}Version of April 10, 2018

[†]Università di Pavia, Dipartimento di Matematica “F. Casorati”, Via A. Ferrata 1, 27100 Pavia, Italy.

[‡]IMATI-CNR “Enrico Magenes”, Pavia, Italy.

Emails: monica.montardini01@universitadipavia.it, {giancarlo.sangalli, mattia.tani}@unipv.it

In this paper the problem of interest is the Stokes system. We consider in particular two well-known isogeometric discretizations for which stability and convergence is known. One is the extension of the Taylor-Hood element, which is *inf-sup* stable, see [8, 7, 9, 10, 11]. The other is the extension of the Raviart-Thomas element, which is stable and structure-preserving, in the sense that the discrete solution is pointwise divergence-free; see [9, 12] (and [13, 14] for its extension to Navier-Stokes). Both allow for arbitrary degree and regularity, in the spirit of the k -method.

The k -method is not costless: the computational cost per degree-of-freedom when dealing with the k -method linear system grows as the degree and regularity increase. In this paper we focus on the cost of solving the system, which is only one part of the problem (the other important part is the formation of the system matrix, which is also an active research field). Linear solvers that are developed for finite elements (e.g., direct [15], iterative multilevel [16]) work well for low-degree isogeometric analysis but the computational performance deteriorates for the high-degree k -method. Recently, papers have appeared with preconditioners that behave robustly for the isogeometric k -method: [17] adopts a domain-decomposition approach, [18] and [19] are based on the multigrid idea (in particular, the latter contains a proof of robustness, based on the theory of [19]), and finally [20], which uses a direct solver at the preconditioner stage, and takes advantage of the tensor-product structure of the multivariate spline spaces. All these papers deal with the Poisson problem.

Isogeometric preconditioners for the Stokes system have also been studied in recent papers: [21, 22] consider block-diagonal and block-triangular preconditioners combined to black-box solvers (either algebraic-multigrid or incomplete factorization); [23] studies the domain-decomposition FETI-DP strategy; [24] focuses on a multigrid strategy; another multigrid approach, which extends the results of [19], can be found in [25].

In the present work, for both Taylor-Hood and Raviart-Thomas isogeometric discretizations of the Stokes system, we consider preconditioners having the classical block structure (see [26]) and using direct solvers to invert the diagonal blocks.

In the simplest approach, our pressure Schur complement preconditioner is the pressure mass matrix in parametric coordinates, which is solved by exploiting its Kronecker structure. Moreover, our preconditioner for the velocity blocks is a component-wise Laplacian in parametric coordinates, and its solution is the solution of a Sylvester-like equation. The latter equation is well studied in the numerical linear algebra community (see for example the overview [27]); among many methods, following [20] we adopt a direct solver named Fast Diagonalization (FD) method, see [28, 29].

An important problem we have to face is the treatment of the geometry parametrization. The simplest approach outlined above does not incorporate any geometry information in the preconditioner, causing a significant loss of efficiency on complex geometry parametrizations. To overcome this limitation, we propose a modification of the preconditioner for a partial inclusion of the geometry information, without increasing its computational cost. Even though the mathematical analysis of this modification is postponed to a later work, in our numerical benchmarking we show the clear benefits of this approach. Indeed, we show theoretically and numerically that our preconditioner is robust with respect to the mesh size h and spline degree p , both for the isogeometric Taylor-Hood and Raviart-Thomas methods. While previous papers considered low-degree splines only (typically quadratics and cubics), we are motivated to consider higher degrees in our tests (up to degree 6 for the velocity and 5 for the pressure, for memory constraints) by the fact that the computational cost of our preconditioner is almost independent of the degree. The iterative solver total computational time is $O(n_{dof}p^3)$, but it is heavily dominated by the matrix-vector multiplication which takes more than the 99% of the overall cost when the pressure degree is 5 and the velocity degree is 6, on a 16^3 elements mesh. In this case our preconditioners is much faster than the alternatives known in literature: for example, about 3 orders of magnitude when comparing to a standard preconditioner based on the incomplete Cholesky factorization, which is known to be an effective choice (see, e.g., [21]).

In conclusion our numerical benchmarks confirm that the proposed preconditioner is very efficient and well suited for the k -method. Further advances in the solver performance can be achieved with a matrix-free approach, that accelerates the matrix-vector multiplication operation, for moderate or large degree. A first step in this research direction is [30].

The outline of the paper is as follows. In Section 2 we give a short review of the Taylor-Hood and Raviart-Thomas isogeometric discretizations for the Stokes system, and summarize the main properties of the Kronecker product. The derivation of the discrete Stokes system is given in Section 3, while in Section 4 we introduce some standard block-structured preconditioners that we will consider in the numerical tests. The core of the paper is Section 5, where we focus on the construction of the preconditioning matrices for the velocity and pressure blocks, discuss their properties and solution strategies. In the Section 6 we propose the modification aimed at improving the preconditioner efficiency by incorporating some information on the geometry parametrization. Numerical results on three different single-patch domains are reported in Section 7. Finally, in Section 8 we draw the conclusions and discuss future directions of research.

2 Preliminaries

2.1 B-splines

In this section we summarize some basic concepts of B-spline based isogeometric analysis, referring to [2] for the details.

Given m and p two positive integers, we introduce a *knot vector* $\Xi := \{0 = \xi_1 \leq \dots \leq \xi_{m+p+1} = 1\}$ and the associated *breakpoint vector* $\mathcal{Z} := \{\zeta_1, \dots, \zeta_s\}$, which contains knots without repetitions. We use *open* knot vectors, i.e. we suppose $\xi_1 = \dots = \xi_{p+1} = 0$ and $\xi_m = \dots = \xi_{m+p+1} = 1$.

Then, according to Cox-De Boor recursion formulas [31], we define univariate B-splines as:

for $p = 0$:

$$\hat{b}_{\alpha,i}^0(\eta) = \begin{cases} 1 & \text{if } \xi_i \leq \eta < \xi_{i+1}, \\ 0 & \text{otherwise;} \end{cases}$$

for $p \geq 1$:

$$\hat{b}_{\alpha,i}^p(\eta) = \begin{cases} \frac{\eta - \xi_i}{\xi_{i+p} - \xi_i} \hat{b}_{\alpha,i}^{p-1}(\eta) + \frac{\xi_{i+p+1} - \eta}{\xi_{i+p+1} - \xi_{i+1}} \hat{b}_{\alpha,i+1}^{p-1}(\eta) & \text{if } \xi_i \leq \eta < \xi_{i+p+1}, \\ 0 & \text{otherwise,} \end{cases}$$

where we adopt the convention $0/0 = 0$ and $\alpha := \{-1, \alpha_2, \dots, \alpha_{s-1}, -1\}$ represents the *regularity vector*. Therefore, B-splines are piecewise polynomials with α_i continuous derivatives at ζ_i . The sum of the continuity and the multiplicity at a breakpoint is equal to the degree p , see [2].

The corresponding *univariate spline space* is defined as

$$\hat{\mathcal{S}}_{\alpha}^p := \text{span}\{\hat{b}_{\alpha,i}^p\}_{i=1}^m.$$

To simplify the notation, we assume throughout this paper that the knot vector is *uniform*, i.e. with equally spaced breakpoints, and the mesh size is denoted by h . For the same reason, we consider uniform regularity $\alpha = \{-1, \alpha, \dots, \alpha, -1\}$. Then we use the notation $\hat{\mathcal{S}}_{\alpha}^p$, $\hat{b}_{\alpha,i}^p$ and set $m_{\alpha}^p := m = \dim(\hat{\mathcal{S}}_{\alpha}^p)$. The extension of this framework to non-uniform knot vectors and arbitrary regularity is trivial (see, in this context, [11, Remark 4.4] and [7]) and is considered in our numerical tests.

We consider multivariate B-splines as tensor-products of univariate B-splines. For 3D problems, the case we address in this paper, the univariate knot vectors $\Xi_l := \{\xi_{l,1}, \dots, \xi_{l, m_{\alpha_l}^{p_l} + p_l + 1}\}$ for $l = 1, 2, 3$ and degree indices $\mathbf{p} = (p_1, p_2, p_3)$ are given and, for a multi-index $\mathbf{i} = (i_1, i_2, i_3)$, the multivariate B-spline is defined as

$$\hat{B}_{\alpha, \mathbf{i}}^{\mathbf{p}}(\boldsymbol{\eta}) := \hat{b}_{\alpha_1, i_1}^{p_1}(\eta_1) \hat{b}_{\alpha_2, i_2}^{p_2}(\eta_2) \hat{b}_{\alpha_3, i_3}^{p_3}(\eta_3)$$

where $\boldsymbol{\eta} = (\eta_1, \eta_2, \eta_3)$, and the *multivariate spline space* as

$$\hat{S}_{\alpha_1, \alpha_2, \alpha_3}^{p_1, p_2, p_3} := \hat{S}_{\alpha_1}^{p_1} \otimes \hat{S}_{\alpha_2}^{p_2} \otimes \hat{S}_{\alpha_3}^{p_3} = \text{span}\{\hat{B}_{\alpha, \mathbf{i}}^{\mathbf{p}} \mid i_k = 1, \dots, m_{\alpha_k}^{p_k}; k = 1, 2, 3\}.$$

Throughout this paper, we refer to *spline spaces* as spaces of splines defined on the parametric domain $\hat{\Omega} := [0, 1]^3$.

2.2 Isogeometric spaces

Let the computational domain $\Omega \subset \mathbb{R}^3$ be given by a single-patch spline parametrization $\mathbf{G} \in \hat{S}_{\alpha_1, \alpha_2, \alpha_3}^{p, p, p} \times \hat{S}_{\alpha_1, \alpha_2, \alpha_3}^{p, p, p} \times \hat{S}_{\alpha_1, \alpha_2, \alpha_3}^{p, p, p}$ of degree p in each parametric direction. We assume that \mathbf{G} is nonsingular, in the sense that its Jacobian is everywhere invertible.

Isogeometric spaces over Ω are suitable push-forwards, through \mathbf{G} , of spline spaces. In particular, in the context of the Stokes system, we focus on two discretizations of isogeometric spaces that have been proposed in [11] and [7] respectively. Their definition and properties are summarized in this section, see [8, 10, 11, 7, 12] for further details.

2.2.1 Taylor-Hood isogeometric spaces

The Taylor-Hood (TH) spline spaces are defined as

$$\begin{aligned} \hat{V}_h^{TH} &:= \hat{S}_{\alpha_1, \alpha_2, \alpha_3}^{p+1, p+1, p+1} \times \hat{S}_{\alpha_1, \alpha_2, \alpha_3}^{p+1, p+1, p+1} \times \hat{S}_{\alpha_1, \alpha_2, \alpha_3}^{p+1, p+1, p+1} \\ \hat{Q}_h^{TH} &:= \hat{S}_{\alpha_1, \alpha_2, \alpha_3}^{p, p, p}. \end{aligned}$$

For the velocity space we will also need

$$\hat{V}_{h,0}^{TH} := \left\{ \hat{\mathbf{v}}_h \in \hat{V}_h^{TH} \mid \hat{\mathbf{v}}_h = 0 \text{ on } \partial\hat{\Omega} \right\}.$$

A basis for \hat{V}_h^{TH} is

$$\left\{ \mathbf{e}_k \hat{B}_{\alpha, \mathbf{i}}^{p+1} \mid i_l = 1, \dots, m_{\alpha_l}^{p+1}; k, l = 1, 2, 3 \right\}.$$

where $\mathbf{p} + 1 := (p + 1, p + 1, p + 1)$ and \mathbf{e}_k is the k -th canonical basis vector of \mathbb{R}^3 .

A basis for $\hat{V}_{h,0}^{TH}$ is then

$$\left\{ \mathbf{e}_k \hat{B}_{\alpha, \mathbf{i}}^{p+1} \mid i_l = 2, \dots, m_{\alpha_l}^{p+1} - 1; k, l = 1, 2, 3 \right\}. \quad (2.1)$$

To each multi-index \mathbf{i} present in (2.1) we associate a scalar index i , corresponding to the lexicographical ordering of the internal degrees of freedom, such that

$$i = i_1 - 1 + (i_2 - 2)(m_{\alpha_1}^{p+1} - 2) + (i_3 - 2)(m_{\alpha_1}^{p+1} - 2)(m_{\alpha_2}^{p+1} - 2)$$

and, with abuse of notation, we rewrite the basis of $\hat{V}_{h,0}^{TH}$ as

$$\left\{ \mathbf{e}_k \hat{B}_{\alpha,i}^{p+1} \mid i = 1, \dots, n_{V,k}^{TH}; k = 1, 2, 3 \right\},$$

where $n_{V,1}^{TH} = n_{V,2}^{TH} = n_{V,3}^{TH} := (m_{\alpha_1}^{p+1} - 2)(m_{\alpha_2}^{p+1} - 2)(m_{\alpha_3}^{p+1} - 2)$.

A basis for \hat{Q}_h^{TH} is

$$\left\{ \hat{B}_{\alpha,i}^p \mid i_l = 1, \dots, m_{\alpha_l}^p; l = 1, 2, 3 \right\}. \quad (2.2)$$

To each multi-index \mathbf{i} present in (2.2) we associate a scalar index i , corresponding to the lexicographical ordering of the internal degrees of freedom, such that

$$i = i_1 + (i_2 - 1)m_{\alpha_1}^p + (i_3 - 1)m_{\alpha_1}^p m_{\alpha_2}^p \quad (2.3)$$

and, with abuse of notation, we rewrite the basis of \hat{Q}_h^{TH} as

$$\left\{ \hat{B}_{\alpha,i}^p \mid i = 1, \dots, n_Q^{TH} \right\}, \quad (2.4)$$

where

$$n_Q^{TH} := \dim(\hat{Q}_h^{TH}) = m_{\alpha_1}^p m_{\alpha_2}^p m_{\alpha_3}^p. \quad (2.5)$$

The TH isogeometric spaces are the isoparametric push-forwards (see [11, 7]):

$$V_{h,0}^{TH} := \text{span} \left\{ \phi_i^{k,TH} := \mathbf{e}_k \hat{B}_{\alpha,i}^{p+1} \circ \mathbf{G}^{-1} \mid i = 1, \dots, n_{V,k}^{TH}; k = 1, 2, 3 \right\} \quad (2.6a)$$

$$Q_h^{TH} := \text{span} \left\{ \rho_i^{TH} := \hat{B}_{\alpha,i}^p \circ \mathbf{G}^{-1} \mid i = 1, \dots, n_Q^{TH} \right\}. \quad (2.6b)$$

For the discrete variational formulation of the Stokes system we will also need the space

$$Q_{h,0}^{TH} := \left\{ q \in Q_h^{TH} \mid \int_{\Omega} q \, d\Omega = 0 \right\}. \quad (2.7)$$

2.2.2 Raviart-Thomas isogeometric spaces

The Raviart-Thomas (RT) spline spaces are defined as

$$\begin{aligned} \hat{V}_h^{RT} &:= \hat{\mathcal{S}}_{\alpha_1+1, \alpha_2, \alpha_3}^{p+1, p, p} \times \hat{\mathcal{S}}_{\alpha_1, \alpha_2+1, \alpha_3}^{p, p+1, p} \times \hat{\mathcal{S}}_{\alpha_1, \alpha_2, \alpha_3+1}^{p, p, p+1} \\ \hat{Q}_h^{RT} &:= \hat{\mathcal{S}}_{\alpha_1, \alpha_2, \alpha_3}^{p, p, p}. \end{aligned}$$

For the velocity space we will also need

$$\hat{V}_{h,0}^{RT} := \left\{ \hat{\mathbf{v}}_h \in \hat{V}_h^{RT} \mid \hat{\mathbf{v}}_h \cdot \mathbf{n} = 0 \text{ on } \partial\hat{\Omega} \right\}.$$

A basis for \hat{V}_h^{RT} is

$$\left\{ \mathbf{e}_k \hat{B}_{\alpha+\mathbf{e}_k, \mathbf{i}}^{p+\mathbf{e}_k} \mid i_k = 1, \dots, m_{\alpha_k+1}^{p+1}; i_l = 1, \dots, m_{\alpha_l}^p; l \neq k; l, k = 1, 2, 3 \right\},$$

where $\mathbf{p} + \mathbf{e}_1 = (p + 1, p, p)$, $\mathbf{p} + \mathbf{e}_2 = (p, p + 1, p)$, $\mathbf{p} + \mathbf{e}_3 = (p, p, p + 1)$ and $\boldsymbol{\alpha} + \mathbf{e}_1 = (\alpha_1 + 1, \alpha_2, \alpha_3)$, $\boldsymbol{\alpha} + \mathbf{e}_2 = (\alpha_1, \alpha_2 + 1, \alpha_3)$, $\boldsymbol{\alpha} + \mathbf{e}_3 = (\alpha_1, \alpha_2, \alpha_3 + 1)$.

A basis for $\hat{V}_{h,0}^{RT}$ is then

$$\left\{ \mathbf{e}_k \hat{B}_{\boldsymbol{\alpha} + \mathbf{e}_k, i}^{\mathbf{p} + \mathbf{e}_k} \mid i_k = 2, \dots, m_{\alpha_k + 1}^{p+1} - 1; i_l = 1, \dots, m_{\alpha_l}^p; l \neq k; l, k = 1, 2, 3 \right\}. \quad (2.8)$$

To each multi-index \mathbf{i} present in (2.8) we associate a scalar index i , corresponding to the lexicographical ordering of the internal degrees of freedom, such that

$$\begin{aligned} \text{for } k = 1 \quad i &= i_1 - 1 + (i_2 - 1)(m_{\alpha_1 + 1}^{p+1} - 2) + (i_3 - 1)(m_{\alpha_1 + 1}^{p+1} - 2)m_{\alpha_2}^p, \\ \text{for } k = 2 \quad i &= i_1 + (i_2 - 2)m_{\alpha_1}^p + (i_3 - 1)m_{\alpha_1}^p(m_{\alpha_2 + 1}^{p+1} - 2), \\ \text{for } k = 3 \quad i &= i_1 + (i_2 - 1)m_{\alpha_1}^p + (i_3 - 2)m_{\alpha_1}^p m_{\alpha_2}^p \end{aligned}$$

and, with abuse of notation, we rewrite the basis of $\hat{V}_{h,0}^{RT}$ as

$$\left\{ \mathbf{e}_k \hat{B}_{\boldsymbol{\alpha} + \mathbf{e}_k, i}^{\mathbf{p} + \mathbf{e}_k} \mid i = 1, \dots, n_{V,k}^{RT}; k = 1, 2, 3 \right\}, \quad (2.9)$$

where

$$n_{V,1}^{RT} = (m_{\alpha_1 + 1}^{p+1} - 2)m_{\alpha_2}^p m_{\alpha_3}^p, \quad n_{V,2}^{RT} = m_{\alpha_1}^p (m_{\alpha_2 + 1}^{p+1} - 2)m_{\alpha_3}^p, \quad n_{V,3}^{RT} = m_{\alpha_1}^p m_{\alpha_2}^p (m_{\alpha_3 + 1}^{p+1} - 2).$$

As $\hat{Q}_h^{RT} = \hat{Q}_h^{TH}$, a basis for \hat{Q}_h^{RT} is (2.4) and its dimension is denoted by $n_Q^{RT} = n_Q^{TH} = n_Q$ (cfr. (2.5)).

The RT isogeometric spaces are defined by suitable push-forwards:

$$V_{h,0}^{RT} := \text{span} \left\{ \phi_i^{k,RT} := \left((\det(J_{\mathcal{G}}))^{-1} J_{\mathcal{G}} \mathbf{e}_k \hat{B}_{\boldsymbol{\alpha} + \mathbf{e}_k, i}^{\mathbf{p} + \mathbf{e}_k} \right) \circ \mathbf{G}^{-1} \mid i = 1, \dots, n_{V,k}^{RT}; k = 1, 2, 3 \right\} \quad (2.10a)$$

$$Q_h^{RT} := \text{span} \left\{ \rho_i^{RT} := \left((\det(J_{\mathcal{G}}))^{-1} \hat{B}_{\boldsymbol{\alpha}, i}^{\mathbf{p}} \right) \circ \mathbf{G}^{-1} \mid i = 1, \dots, n_Q^{RT} \right\}. \quad (2.10b)$$

The push-forward employed for $V_{h,0}^{RT}$ is the Piola transform and its use is important to assure inf-sup stability, see [7] and Section 3.

We remark that although in the parametric domain $\hat{Q}_h^{RT} = \hat{Q}_h^{TH}$, in general $Q_h^{RT} \neq Q_h^{TH}$.

For the discrete variational formulation of the Stokes system we will also need the space

$$Q_{h,0}^{RT} := \left\{ q \in Q_h^{RT} \mid \int_{\Omega} q \, d\Omega = 0 \right\}. \quad (2.11)$$

2.3 The Kronecker product

We restrict to the case of square matrices and we consider $A \in \mathbb{R}^{n_1 \times n_1}$, $B \in \mathbb{R}^{n_2 \times n_2}$ and $C \in \mathbb{R}^{n_3 \times n_3}$. The entries of the matrix A are denoted with $[A]_{i,j}$.

The *Kronecker product* between A and B is defined as

$$A \otimes B := \begin{bmatrix} [A]_{1,1} B & \dots & [A]_{1,n_1} B \\ \vdots & \ddots & \vdots \\ [A]_{n_1,1} B & \dots & [A]_{n_1,n_1} B \end{bmatrix} \in \mathbb{R}^{n_1 n_2 \times n_1 n_2}.$$

This operation is associative: $A \otimes B \otimes C = (A \otimes B) \otimes C = A \otimes (B \otimes C)$.

Given a tensor $\mathbb{W} \in \mathbb{R}^{n_1 \times n_2 \times n_3}$, the *vec* operator converts \mathbb{W} to a vector $\text{vec}(\mathbb{W}) \in \mathbb{R}^{n_1 n_2 n_3}$ as

$$[\text{vec}(\mathbb{W})]_i := [\mathbb{W}]_{i_1, i_2, i_3}$$

where $i = i_1 + (i_2 - 1)n_1 + (i_3 - 1)n_1 n_2$, for $i_k = 1, \dots, n_k$ and $k = 1, 2, 3$.

Let $Y_m \in \mathbb{R}^{i \times n_m}$ for $m = 1, 2, 3$ be three matrices. The *m-mode* product \times_m gives the following tensors

$$\begin{aligned} [\mathbb{W} \times_1 Y_1]_{i_1, i_2, i_3} &:= \sum_{k=1}^{n_1} [Y_1]_{i_1, k} [\mathbb{W}]_{k, i_2, i_3} & [\mathbb{W} \times_2 Y_2]_{i_1, i_2, i_3} &:= \sum_{k=1}^{n_2} [Y_2]_{i_2, k} [\mathbb{W}]_{i_1, k, i_3} \\ [\mathbb{W} \times_3 Y_3]_{i_1, i_2, i_3} &:= \sum_{k=1}^{n_3} [Y_3]_{i_3, k} [\mathbb{W}]_{i_1, i_2, k}. \end{aligned}$$

See [32] for more details.

Being primarily interested in 3D problems, we will deal with matrices of the form $A \otimes B \otimes C$. We will need the following properties:

- It holds

$$(A \otimes B \otimes C)^T = A^T \otimes B^T \otimes C^T. \quad (2.12)$$

In particular, if A , B and C are symmetric, then also $A \otimes B \otimes C$ is symmetric.

- If A , B and C are nonsingular, then

$$(A \otimes B \otimes C)^{-1} = A^{-1} \otimes B^{-1} \otimes C^{-1}. \quad (2.13)$$

- Let $\lambda_1, \dots, \lambda_{n_1}$ denote the eigenvalues of A , μ_1, \dots, μ_{n_2} , denote the eigenvalues of B and ν_1, \dots, ν_{n_3} denote the eigenvalues of C . Then the eigenvalues of $A \otimes B \otimes C$ are $\lambda_i \mu_j \nu_k$, $i = 1, \dots, n_1$, $j = 1, \dots, n_2$, $k = 1, \dots, n_3$. In particular, if A , B and C are positive definite, then also $A \otimes B \otimes C$ is positive definite.

- If $\mathbb{X} \in \mathbb{R}^{n_1 \times n_2 \times n_3}$, then

$$(A \otimes B \otimes C) \text{vec}(\mathbb{X}) = \text{vec}(\mathbb{X} \times_1 A \times_2 B \times_3 C). \quad (2.14)$$

Thanks to this property the matrix $A \otimes B \otimes C$ does not need to be formed to compute a matrix-vector product, resulting in a significant saving of memory and floating point operations (FLOPs).

- It holds (from (2.13) and (2.14)):

$$(A \otimes B \otimes C)^{-1} \text{vec}(\mathbb{X}) = \text{vec}(\mathbb{X} \times_1 A^{-1} \times_2 B^{-1} \times_3 C^{-1}). \quad (2.15)$$

3 Isogeometric analysis of the Stokes system

The Stokes system reads as

$$\begin{aligned} -\nabla \cdot (2\nu \nabla^s \mathbf{u}) + \nabla p &= \mathbf{f} & \text{in } \Omega \\ \nabla \cdot \mathbf{u} &= 0 & \text{in } \Omega \end{aligned}$$

where $\nabla^s = \frac{1}{2}(\nabla + \nabla^T)$, \mathbf{u} is the velocity, p is the scalar pressure and $\nu > 0$ is the kinematic viscosity. We assume $\nu \in L^\infty(\Omega)$ and $\mathbf{f} \in \mathbf{L}^2(\Omega)$. We consider no-slip boundary conditions, that is we impose $\mathbf{u} = 0$ on $\partial\Omega$. The pressure is determined up to a constant.

The standard (mixed) variational formulation of the problem reads: find $\mathbf{u} \in \mathbf{H}_0^1(\Omega) := \{\mathbf{v} \in \mathbf{H}^1(\Omega) \mid \mathbf{v} = 0 \text{ on } \partial\Omega\}$ and $p \in L_0^2(\Omega) := \{q \in L^2(\Omega) \mid \int_\Omega q \, d\Omega = 0\}$ such that

$$a(\mathbf{u}, \mathbf{v}) + b(\mathbf{u}, p) = (\mathbf{f}, \mathbf{v})_{L^2} \quad \forall \mathbf{v} \in \mathbf{H}_0^1(\Omega) \quad (3.1a)$$

$$b(\mathbf{u}, q) = 0 \quad \forall q \in L_0^2(\Omega), \quad (3.1b)$$

where $(\cdot, \cdot)_{L^2}$ denotes the L^2 scalar product while the bilinear forms $a(\cdot, \cdot)$ and $b(\cdot, \cdot)$ are defined as

$$a(\mathbf{w}, \mathbf{v}) = \int_\Omega 2\nu \nabla^s \mathbf{w} : \nabla^s \mathbf{v} \, d\Omega \quad (3.2)$$

$$b(\mathbf{v}, q) = - \int_\Omega q \nabla \cdot \mathbf{v} \, d\Omega.$$

The isogeometric Taylor-Hood (TH) discretization of Stokes system is a standard Galerkin method for (3.1) and reads: find $\mathbf{u}_h^{TH} \in V_{h,0}^{TH}$ and $p_h^{TH} \in Q_{h,0}^{TH}$ such that

$$a(\mathbf{u}_h^{TH}, \mathbf{v}_h) + b(\mathbf{v}_h, p_h^{TH}) = (f, \mathbf{v}_h)_{L^2} \quad \forall \mathbf{v}_h \in V_{h,0}^{TH}, \quad (3.3a)$$

$$b(\mathbf{u}_h^{TH}, q_h) = 0 \quad \forall q_h \in Q_{h,0}^{TH}, \quad (3.3b)$$

where $V_{h,0}^{TH}$ and $Q_{h,0}^{TH}$ are defined as (2.6a) and (2.7). A detailed analysis on the well posedness of this problem can be found in [8, 10, 11].

The isogeometric Raviart-Thomas (RT) discretization we adopt is based on a Nitsche formulation for the weak imposition of the tangential Dirichlet boundary condition to ensure stability (see [12]).

The method reads: find $\mathbf{u}_h^{RT} \in V_{h,0}^{RT}$ and $p_h^{RT} \in Q_{h,0}^{RT}$ such that

$$a(\mathbf{u}_h^{RT}, \mathbf{v}_h) + \sigma(\mathbf{u}_h^{RT}, \mathbf{v}_h) + b(\mathbf{v}_h, p_h^{RT}) = (f, \mathbf{v}_h)_{L^2} \quad \forall \mathbf{v}_h \in V_{h,0}^{RT}, \quad (3.4a)$$

$$b(\mathbf{u}_h^{RT}, q_h) = 0 \quad \forall q_h \in Q_{h,0}^{RT}, \quad (3.4b)$$

where $V_{h,0}^{RT}$ and $Q_{h,0}^{RT}$ are defined as (2.10a) and (2.11) and the bilinear form $\sigma(\cdot, \cdot)$ is defined as

$$\sigma(\mathbf{w}_h, \mathbf{v}_h) := \int_{\partial\Omega} 2\nu \left[\frac{C_{pen}}{h} \mathbf{w}_h \cdot \mathbf{v}_h - ((\nabla^s \mathbf{w}_h) \mathbf{n}) \cdot \mathbf{v}_h - ((\nabla^s \mathbf{v}_h) \mathbf{n}) \cdot \mathbf{w}_h \right] \, d\Gamma, \quad (3.5)$$

with $C_{pen} > 0$ a penalty parameter. The well-posedness of RT discretization for Stokes problem and the choice of C_{pen} are analysed in [12].

In practice, we build the linear system by replacing $Q_{h,0}^{TH}$ and $Q_{h,0}^{RT}$ by Q_h^{TH} and Q_h^{RT} , respectively. This means that we do not incorporate the zero-mean-value constraint into the pressure space, since this will be taken care of by the Krylov iterative solver later.

Then, the discrete Stokes system matrix is

$$\mathcal{A} = \begin{bmatrix} A & B^T \\ B & 0 \end{bmatrix}, \quad (3.6)$$

where

$$A = \begin{bmatrix} A_{11} & A_{12} & A_{13} \\ A_{21} & A_{22} & A_{23} \\ A_{31} & A_{32} & A_{33} \end{bmatrix}, \quad B = [B_1 \ B_2 \ B_3],$$

and for TH discretization, $i = 1, \dots, n_{V,r}^{TH}$, $j = 1, \dots, n_{V,s}^{TH}$, $r, s = 1, 2, 3$ and $l = 1, \dots, n_Q$

$$\begin{aligned} [A_{rs}^{TH}]_{i,j} &:= a(\phi_i^{r,TH}, \phi_j^{s,TH}), \\ [B_r^{TH}]_{l,j} &:= b(\phi_j^{r,TH}, \rho_l^{TH}), \end{aligned}$$

while for RT discretization, $i = 1, \dots, n_{V,r}^{RT}$, $j = 1, \dots, n_{V,s}^{RT}$, $r, s = 1, 2, 3$ and $l = 1, \dots, n_Q$

$$\begin{aligned} [A_{rs}^{RT}]_{i,j} &:= a(\phi_i^{r,RT}, \phi_j^{s,RT}) + \sigma(\phi_i^{r,RT}, \phi_j^{s,RT}), \\ [B_r^{RT}]_{l,j} &:= b(\phi_j^{r,RT}, \rho_l^{RT}), \end{aligned}$$

referring to Section 2.2 for the notations of the basis.

In particular we have that for $k = 1, 2, 3$

$$[A_{kk}^{TH}]_{i,j} = \int_{\hat{\Omega}} \left(\nabla \hat{B}_{\alpha,i}^{p+1} \right)^T \mathfrak{e}_k^{TH} \nabla \hat{B}_{\alpha,j}^{p+1} d\boldsymbol{\eta}, \quad (3.7)$$

where

$$\mathfrak{e}_k^{TH}(\boldsymbol{\eta}) = \nu(J_{\mathbf{G}}^{-1} J_{\mathbf{G}}^{-T} + D_k D_k^T) |\det(J_{\mathbf{G}})| \quad (3.8)$$

and $D_k := J_{\mathbf{G}}^{-1} \mathbf{e}_k$, while

$$\begin{aligned} [A_{kk}^{RT}]_{i,j} &:= \int_{\hat{\Omega}} \left(\nabla \hat{B}_{\alpha+\mathbf{e}_k,i}^{p+\mathbf{e}_k} \right)^T \mathfrak{e}_k^{RT} \nabla \hat{B}_{\alpha+\mathbf{e}_k,j}^{p+\mathbf{e}_k} d\boldsymbol{\eta} + \sigma \left(\left(\tilde{J}_{\mathbf{G}} \mathbf{e}_k \hat{B}_{\alpha+\mathbf{e}_k,i}^{p+\mathbf{e}_k} \right) \circ \mathbf{G}^{-1}, \left(\tilde{J}_{\mathbf{G}} \mathbf{e}_k \hat{B}_{\alpha+\mathbf{e}_k,j}^{p+\mathbf{e}_k} \right) \circ \mathbf{G}^{-1} \right) \\ &\quad + \int_{[0,1]^3} 2\nu \left\{ \left[R_k \left(\nabla \hat{B}_{\alpha+\mathbf{e}_k,i}^{p+\mathbf{e}_k} J_{\mathbf{G}}^{-1} \right) \right]^s : \left[(\mathbb{H}_{\mathbf{G}} \mathbf{e}_k \hat{B}_{\alpha+\mathbf{e}_k,j}^{p+\mathbf{e}_k}) J_{\mathbf{G}}^{-1} \right]^s \right. \\ &\quad \left. + \left[(\mathbb{H}_{\mathbf{G}} \mathbf{e}_k \hat{B}_{\alpha+\mathbf{e}_k,i}^{p+\mathbf{e}_k}) J_{\mathbf{G}}^{-1} \right]^s : \left[R_k \left(\nabla \hat{B}_{\alpha+\mathbf{e}_k,j}^{p+\mathbf{e}_k} J_{\mathbf{G}}^{-1} \right) \right]^s \right. \\ &\quad \left. + \left\| \left[(\mathbb{H}_{\mathbf{G}} \mathbf{e}_k \hat{B}_{\alpha+\mathbf{e}_k,j}^{p+\mathbf{e}_k}) J_{\mathbf{G}}^{-1} \right]^s \right\|_F^2 \right\} |\det(J_{\mathbf{G}})| d\boldsymbol{\eta}, \quad (3.9) \end{aligned}$$

where

$$\mathfrak{e}_k^{RT}(\boldsymbol{\eta}) = \nu |\det(J_{\mathbf{G}})| J_{\mathbf{G}}^{-1} (\|R_k\|_2^2 I + R_k R_k^T) J_{\mathbf{G}}^{-T}, \quad (3.10)$$

$\tilde{J}_{\mathbf{G}} := (\det(J_{\mathbf{G}}))^{-1} J_{\mathbf{G}}$, $R_k := \tilde{J}_{\mathbf{G}} \mathbf{e}_k$ and $\mathbb{H}_{\mathbf{G}}$ is the (trivariate) Hessian tensor $\mathbb{H}_{\mathbf{G}} := \nabla \tilde{J}_{\mathbf{G}}$, with the convention that, for a given vector $\mathbf{w} \in \mathbb{R}^3$,

$$\mathbb{H}_{\mathbf{G}} \mathbf{w} := \left[\left(\partial_{\eta_1} \tilde{J}_{\mathbf{G}} \right) \mathbf{w}, \quad \left(\partial_{\eta_2} \tilde{J}_{\mathbf{G}} \right) \mathbf{w}, \quad \left(\partial_{\eta_3} \tilde{J}_{\mathbf{G}} \right) \mathbf{w} \right].$$

Here and throughout, $\|\cdot\|_2$ denotes the Euclidean vector norm and the induced matrix norm, $\|\cdot\|_F$ refers to the Frobenius matrix norm and $[\cdot]^s$ denotes the symmetric part. Note that the last integral in (3.9) is zero when \mathbf{G} is the identity map.

4 Preconditioners for the whole system

In this section we introduce the preconditioning strategies that we consider in our numerical tests. In what follows P_V represents a preconditioning matrix for the block A and P_Q a preconditioning matrix for S , where

$$S = BA^{-1}B^T \quad (4.1)$$

is the (negative) Schur complement.

Once P_V and P_Q are constructed (this will be discussed in the next section), one can set up suitable preconditioners to be used in the context of Krylov iterative methods [33, 26, 34, 35]. We select three approaches.

In the first one, we consider the block diagonal preconditioner [36]

$$\mathcal{P}_D = \begin{bmatrix} P_V & 0 \\ 0 & P_Q \end{bmatrix}, \quad (4.2)$$

which, being symmetric and positive definite, preserves the symmetry of the problem. Therefore it can be coupled with a method for symmetric systems such as MINRES [37]. In the other two approaches, we respectively consider the block triangular [36] and constrained [38] preconditioners

$$\mathcal{P}_T = \begin{bmatrix} P_V & B^T \\ 0 & -P_Q \end{bmatrix} \quad (4.3)$$

and

$$\mathcal{P}_C = \begin{bmatrix} P_V & B^T \\ B & BP_V^{-1}B^T - P_Q \end{bmatrix}, \quad (4.4)$$

both coupled with the GMRES method [39]. We remark that \mathcal{P}_C^{-1} can be applied efficiently thanks to the factorization

$$\mathcal{P}_C^{-1} = \begin{bmatrix} I & -P_V^{-1}B^T \\ 0 & I \end{bmatrix} \begin{bmatrix} I & 0 \\ 0 & -P_Q^{-1} \end{bmatrix} \begin{bmatrix} I & 0 \\ -B & I \end{bmatrix} \begin{bmatrix} P_V^{-1} & 0 \\ 0 & I \end{bmatrix},$$

where, here and throughout the paper, I denotes the identity matrix of conforming order.

5 Preconditioners for P_V and P_Q : the simple choice

Our choice for the preconditioning block P_V has a block diagonal structure:

$$P_V := \begin{bmatrix} P_{V,1} & 0 & 0 \\ 0 & P_{V,2} & 0 \\ 0 & 0 & P_{V,3} \end{bmatrix}; \quad (5.1)$$

the blocks $P_{V,k}$ are a simplified version of to the blocks A_{kk} where the geometry map and the kinematic viscosity are replaced by the identity map and identity function, respectively. In other words, analogously to (3.2) and (3.5), we define in the parametric domain

$$\hat{a}(\hat{\mathbf{w}}, \hat{\mathbf{v}}) := \int_{\hat{\Omega}} 2 \nabla^s \hat{\mathbf{w}} : \nabla^s \hat{\mathbf{v}} \, d\hat{\Omega},$$

$$\hat{\sigma}(\hat{\mathbf{w}}, \hat{\mathbf{v}}) := \int_{\partial\hat{\Omega}} 2 \left[\frac{C_{pen}}{h} \hat{\mathbf{w}} \cdot \hat{\mathbf{v}} - ((\nabla^s \hat{\mathbf{w}}) \hat{\mathbf{n}}) \cdot \hat{\mathbf{v}} - ((\nabla^s \hat{\mathbf{v}}) \hat{\mathbf{n}}) \cdot \hat{\mathbf{w}} \right] d\hat{\Gamma},$$

where $\hat{\mathbf{n}}$ is the exterior normal to the boundary $\partial\hat{\Omega}$. Therefore for TH discretization, according to (3.7), for $i, j = 1, \dots, n_{V,k}^{TH}$ and $k = 1, 2, 3$ we define

$$[P_{V,k}^{TH}]_{i,j} := \hat{a}(\mathbf{e}_k \hat{B}_{\alpha,i}^{p+1}, \mathbf{e}_k \hat{B}_{\alpha,j}^{p+1}) = \int_{\hat{\Omega}} \left(\nabla \hat{B}_{\alpha,i}^{p+1} \right)^T \mathfrak{T}_k \nabla \hat{B}_{\alpha,j}^{p+1} d\eta, \quad (5.2)$$

where $\mathfrak{T}_k = I + \mathbf{e}_k \mathbf{e}_k^T$, while for RT discretization, according to (3.9), for $i, j = 1, \dots, n_{V,k}^{RT}$ and $k = 1, 2, 3$ we define

$$\begin{aligned} [P_{V,k}^{RT}]_{i,j} &:= \hat{a}(\mathbf{e}_k \hat{B}_{\alpha+\mathbf{e}_k,i}^{p+\mathbf{e}_k}, \mathbf{e}_k \hat{B}_{\alpha+\mathbf{e}_k,j}^{p+\mathbf{e}_k}) + \hat{\sigma} \left(\mathbf{e}_k \hat{B}_{\alpha+\mathbf{e}_k,i}^{p+\mathbf{e}_k}, \mathbf{e}_k \hat{B}_{\alpha+\mathbf{e}_k,j}^{p+\mathbf{e}_k} \right) \\ &= \int_{\hat{\Omega}} \left(\nabla \hat{B}_{\alpha+\mathbf{e}_k,i}^{p+\mathbf{e}_k} \right)^T \mathfrak{T}_k \nabla \hat{B}_{\alpha+\mathbf{e}_k,j}^{p+\mathbf{e}_k} d\eta + \hat{\sigma} \left(\mathbf{e}_k \hat{B}_{\alpha+\mathbf{e}_k,i}^{p+\mathbf{e}_k}, \mathbf{e}_k \hat{B}_{\alpha+\mathbf{e}_k,j}^{p+\mathbf{e}_k} \right). \end{aligned} \quad (5.3)$$

Exploiting the tensor product structure of the basis functions, we can write

$$P_{V,1}^{TH} = K_3^{TH} \otimes M_2^{TH} \otimes M_1^{TH} + M_3^{TH} \otimes K_2^{TH} \otimes M_1^{TH} + 2M_3^{TH} \otimes M_2^{TH} \otimes K_1^{TH}, \quad (5.4a)$$

$$P_{V,2}^{TH} = K_3^{TH} \otimes M_2^{TH} \otimes M_1^{TH} + 2M_3^{TH} \otimes K_2^{TH} \otimes M_1^{TH} + M_3^{TH} \otimes M_2^{TH} \otimes K_1^{TH}, \quad (5.4b)$$

$$P_{V,3}^{TH} = 2K_3^{TH} \otimes M_2^{TH} \otimes M_1^{TH} + M_3^{TH} \otimes K_2^{TH} \otimes M_1^{TH} + M_3^{TH} \otimes M_2^{TH} \otimes K_1^{TH}, \quad (5.4c)$$

and

$$P_{V,1}^{RT} = \tilde{K}_3^{RT} \otimes \tilde{M}_2^{RT} \otimes \tilde{M}_1^{RT} + \tilde{M}_3^{RT} \otimes \tilde{K}_2^{RT} \otimes \tilde{M}_1^{RT} + 2\tilde{M}_3^{RT} \otimes \tilde{M}_2^{RT} \otimes \tilde{K}_1^{RT}, \quad (5.5a)$$

$$P_{V,2}^{RT} = \tilde{K}_3^{RT} \otimes \tilde{M}_2^{RT} \otimes \tilde{M}_1^{RT} + 2\tilde{M}_3^{RT} \otimes \tilde{K}_2^{RT} \otimes \tilde{M}_1^{RT} + \tilde{M}_3^{RT} \otimes \tilde{M}_2^{RT} \otimes \tilde{K}_1^{RT}, \quad (5.5b)$$

$$P_{V,3}^{RT} = 2\tilde{K}_3^{RT} \otimes \tilde{M}_2^{RT} \otimes \tilde{M}_1^{RT} + \tilde{M}_3^{RT} \otimes \tilde{K}_2^{RT} \otimes \tilde{M}_1^{RT} + \tilde{M}_3^{RT} \otimes \tilde{M}_2^{RT} \otimes \tilde{K}_1^{RT}, \quad (5.5c)$$

where for $k = 1, 2, 3$ the univariate matrix factors are

$$[K_k^{TH}]_{l,s} = \int_{[0,1]} (\hat{b}_{\alpha_k,i}^{p+1})'(\eta_k) (\hat{b}_{\alpha_k,s}^{p+1})'(\eta_k) d\eta_k,$$

$$[M_k^{TH}]_{l,s} = \int_{[0,1]} \hat{b}_{\alpha_k,l}^{p+1}(\eta_k) \hat{b}_{\alpha_k,s}^{p+1}(\eta_k) d\eta_k,$$

for $l, s = 2, \dots, m_{\alpha_k}^{p+1} - 1$, and

$$[K_k^{RT}]_{l,s} = \int_{[0,1]} (\hat{b}_{\alpha_k+1,l}^{p+1})'(\eta_k) (\hat{b}_{\alpha_k+1,s}^{p+1})'(\eta_k) d\eta_k,$$

$$[M_k^{RT}]_{l,s} = \int_{[0,1]} \hat{b}_{\alpha_k+1,l}^{p+1}(\eta_k) \hat{b}_{\alpha_k+1,s}^{p+1}(\eta_k) d\eta_k,$$

for $l, s = 2, \dots, m_{\alpha_k+1}^{p+1} - 1$, and finally

$$\begin{aligned} \left[\widetilde{K}_k^{RT} \right]_{l,s} &= \int_{[0,1]} (\hat{b}_{\alpha_k,l}^p)'(\eta_k) (\hat{b}_{\alpha_k,s}^p)'(\eta_k) d\eta_k \\ &\quad - \left[(\hat{b}_{\alpha_k,l}^p)'(1) \hat{b}_{\alpha_k,s}^p(1) - (\hat{b}_{\alpha_k,l}^p)'(0) \hat{b}_{\alpha_k,s}^p(0) + (\hat{b}_{\alpha_k,s}^p)'(1) \hat{b}_{\alpha_k,l}^p(1) \right. \\ &\quad \left. - (\hat{b}_{\alpha_k,s}^p)'(0) \hat{b}_{\alpha_k,l}^p(0) - 2 \frac{C_{pen}}{h} (\hat{b}_{\alpha_k,l}^p(1) \hat{b}_{\alpha_k,s}^p(1) + \hat{b}_{\alpha_k,l}^p(0) \hat{b}_{\alpha_k,s}^p(0)) \right], \\ \left[\widetilde{M}_k^{RT} \right]_{l,s} &= \int_{[0,1]} \hat{b}_{\alpha_k,l}^p(\eta_k) \hat{b}_{\alpha_k,s}^p(\eta_k) d\eta_k \end{aligned}$$

for $l, s = 1, \dots, m_{\alpha_k}^p$.

Now we consider the construction of P_Q . The Schur complement S is spectrally equivalent to the (weighted) pressure mass matrix

$$\begin{aligned} [Q^{TH}]_{i,j} &:= \int_{\Omega} \nu^{-1} \rho_i^{TH} \rho_j^{TH} d\Omega = \int_{\widehat{\Omega}} \nu^{-1} \hat{B}_{\alpha,i}^p \hat{B}_{\alpha,j}^p g^{TH} d\boldsymbol{\eta}, \\ [Q^{RT}]_{i,j} &:= \int_{\Omega} \nu^{-1} \rho_i^{RT} \rho_j^{RT} d\Omega = \int_{\widehat{\Omega}} \nu^{-1} \hat{B}_{\alpha,i}^p \hat{B}_{\alpha,j}^p g^{RT} d\boldsymbol{\eta}, \end{aligned} \quad (5.6)$$

for $i, j = 1, \dots, n_Q$, where $g^{TH}(\boldsymbol{\eta}) := |\det(J_{\mathbf{G}})|$ and $g^{RT}(\boldsymbol{\eta}) := |\det(J_{\mathbf{G}})|^{-1}$. The equivalence holds uniformly with respect to a variable kinematic viscosity ν , see [40]. However, as for P_V , in our simple approach we drop the dependence on ν and the geometry mapping, by selecting:

$$[P_Q^{TH}]_{i,j} := [P_Q^{RT}]_{i,j} := \int_{\widehat{\Omega}} \hat{B}_{\alpha,i}^p \hat{B}_{\alpha,j}^p d\boldsymbol{\eta} \quad i, j = 1, \dots, n_Q;$$

as for (5.2) and (5.3). Exploiting again the tensor product structure of the basis we can write P_Q as

$$P_Q = M_3 \otimes M_2 \otimes M_1, \quad (5.7)$$

where for $k = 1, 2, 3$ and for $l, s = 1, \dots, n_Q$

$$[M_k]_{l,s} = \int_{[0,1]} \hat{b}_{\alpha_k,l}^p(\eta_k) \hat{b}_{\alpha_k,s}^p(\eta_k) d\eta_k.$$

5.1 Spectral properties

A desirable requirement for all the strategies proposed in Section 4 is that P_V and P_Q are spectrally equivalent to A and Q , respectively. We analyse here the spectral properties of $P_V^{-1}A$ and $P_Q^{-1}Q$. We refer to [26, Section 4.2], where such properties are used to derive explicit bounds for the eigenvalues of the preconditioned system $\mathcal{P}^{-1}\mathcal{A}$, in the special case of the block diagonal preconditioner. In particular, if the eigenvalues of $P_V^{-1}A$ and $P_Q^{-1}Q$ are bounded away from 0 and infinity uniformly with respect to h and p , then so are the eigenvalues of the full system.

The bilinear forms $a(\cdot, \cdot)$ and $\hat{a}(\cdot, \cdot)$ satisfy

$$2C_{\text{Korn}} \nu_{\min} |\mathbf{v}|_{\mathbf{H}^1(\Omega)}^2 \leq a(\mathbf{v}, \mathbf{v}) \leq 2\nu_{\max} |\mathbf{v}|_{\mathbf{H}^1(\Omega)}^2 \quad \forall \mathbf{v} \in \mathbf{H}_0^1(\Omega), \quad (5.8)$$

$$2\hat{C}_{\text{Korn}} |\hat{\mathbf{v}}|_{\mathbf{H}^1(\widehat{\Omega})}^2 \leq \hat{a}(\hat{\mathbf{v}}, \hat{\mathbf{v}}) \leq 2|\hat{\mathbf{v}}|_{\mathbf{H}^1(\widehat{\Omega})}^2 \quad \forall \hat{\mathbf{v}} \in \mathbf{H}_0^1(\widehat{\Omega}), \quad (5.9)$$

where $|\cdot|_{\mathbf{H}^1(\cdot)}$ denotes the usual \mathbf{H}^1 -seminorm, C_{Korn} and \hat{C}_{Korn} are the Korn constants (for homogeneous Dirichlet boundary conditions on the whole boundary we have $C_{\text{Korn}} = \hat{C}_{\text{Korn}} = 1/2$, see [41, Section 6.3]) and

$$\nu_{\min} := \inf_{\Omega} \nu, \quad \nu_{\max} := \sup_{\Omega} \nu.$$

We also have that the bilinear forms $a(\cdot, \cdot) + \sigma(\cdot, \cdot)$ and $\hat{a}(\cdot, \cdot) + \hat{\sigma}(\cdot, \cdot)$ in the discrete spaces satisfy

$$C_1 \|\mathbf{v}_h\|_{\mathbf{H}_{pen}^1(\Omega)}^2 \leq a(\mathbf{v}_h, \mathbf{v}_h) + \sigma(\mathbf{v}_h, \mathbf{v}_h) \leq C_2 \|\mathbf{v}_h\|_{\mathbf{H}_{pen}^1(\Omega)}^2 \quad \forall \mathbf{v}_h \in V_{h,0}^{RT}, \quad (5.10)$$

$$\hat{C}_1 \|\hat{\mathbf{v}}_h\|_{\mathbf{H}_{pen}^1(\hat{\Omega})}^2 \leq \hat{a}(\hat{\mathbf{v}}_h, \hat{\mathbf{v}}_h) + \hat{\sigma}(\hat{\mathbf{v}}_h, \hat{\mathbf{v}}_h) \leq \hat{C}_2 \|\hat{\mathbf{v}}_h\|_{\mathbf{H}_{pen}^1(\hat{\Omega})}^2 \quad \forall \hat{\mathbf{v}}_h \in \hat{V}_{h,0}^{RT}, \quad (5.11)$$

where the norm $\|\cdot\|_{\mathbf{H}_{pen}^1(\hat{\Omega})}$ is defined as $\|\cdot\|_{\mathbf{H}_{pen}^1(\hat{\Omega})} := \|\cdot\|_{\mathbf{H}^1(\Omega)} + \frac{C_{pen}}{h} \|\cdot\|_{L^2(\partial\Omega)}$ and C_1 , C_2 , \hat{C}_1 and \hat{C}_2 are constants depending on C_{pen} and on the inverse estimate constants of the discrete spaces $V_{h,0}^{RT}$ and $\hat{V}_{h,0}^{RT}$ respectively: these inequalities follows from [12, Lemma 6.2], [12, Lemma 6.3],[12, Eq. (6.9)] and the equivalence between $\|\cdot\|_{\mathbf{H}_{pen}^1(\hat{\Omega})}$ and $|\cdot|_{\mathbf{H}_{pen}^1(\hat{\Omega})} := |\cdot|_{\mathbf{H}^1(\Omega)} + \frac{C_{pen}}{h} \|\cdot\|_{L^2(\partial\Omega)}$.

We start by proving bounds on the eigenvalues of $P_V^{-1}A$.

Theorem 1. *It holds*

$$\delta \leq \lambda_{\min}(P_V^{-1}A), \quad \lambda_{\max}(P_V^{-1}A) \leq \Delta, \quad (5.12)$$

where δ and Δ are positive constants that do not depend on h or on p .

Proof. We begin with TH discretization case, proving (5.12) for $\delta = \delta^{TH}$ and $\Delta = \Delta^{TH}$. Let $\hat{\mathbf{v}}_h \in \hat{V}_{h,0}^{TH}$ and let $\mathbf{v}_h := \hat{\mathbf{v}}_h \circ \mathbf{G}^{-1} \in V_{h,0}^{TH}$. Moreover, let \mathbf{v} be the coordinate vector of $\hat{\mathbf{v}}_h$ with respect to the basis (2.8). By the Courant-Fischer theorem, (5.12) is equivalent to find δ^{TH} and Δ^{TH} such that

$$\delta^{TH} \leq \frac{\mathbf{v}^T A^{TH} \mathbf{v}}{\mathbf{v}^T P_V^{TH} \mathbf{v}} \leq \Delta^{TH}.$$

Using (5.8), we have

$$2C_{\text{Korn}} \nu_{\min} |\mathbf{v}_h|_{\mathbf{H}^1(\Omega)}^2 \leq \mathbf{v}^T A^{TH} \mathbf{v} \leq 2\nu_{\max} |\mathbf{v}_h|_{\mathbf{H}^1(\Omega)}^2.$$

Using (5.9) and decomposing $\hat{\mathbf{v}}_h = \hat{\mathbf{v}}_{h,1} + \hat{\mathbf{v}}_{h,2} + \hat{\mathbf{v}}_{h,3}$, where $\hat{\mathbf{v}}_{h,k}$ are the cartesian components of $\hat{\mathbf{v}}_h$, we have for $k = 1, 2, 3$,

$$2\hat{C}_{\text{Korn}} |\hat{\mathbf{v}}_{h,k}|_{\mathbf{H}^1(\hat{\Omega})}^2 \leq \hat{a}(\hat{\mathbf{v}}_{h,k}, \hat{\mathbf{v}}_{h,k}) \leq 2|\hat{\mathbf{v}}_{h,k}|_{\mathbf{H}^1(\hat{\Omega})}^2;$$

summing the three bounds above and using $\hat{a}(\hat{\mathbf{v}}_{h,1}, \hat{\mathbf{v}}_{h,1}) + \hat{a}(\hat{\mathbf{v}}_{h,2}, \hat{\mathbf{v}}_{h,2}) + \hat{a}(\hat{\mathbf{v}}_{h,3}, \hat{\mathbf{v}}_{h,3}) = \mathbf{v}^T P_V^{TH} \mathbf{v}$ yields

$$2\hat{C}_{\text{Korn}} |\hat{\mathbf{v}}_h|_{\mathbf{H}^1(\hat{\Omega})}^2 \leq \mathbf{v}^T P_V^{TH} \mathbf{v} \leq 2|\hat{\mathbf{v}}_h|_{\mathbf{H}^1(\hat{\Omega})}^2;$$

in conclusion it suffices to prove

$$\frac{\delta^{TH}}{C_{\text{Korn}} \nu_{\min}} \leq \frac{|\mathbf{v}_h|_{\mathbf{H}^1(\Omega)}^2}{|\hat{\mathbf{v}}_h|_{\mathbf{H}^1(\hat{\Omega})}^2} \leq \frac{\hat{C}_{\text{Korn}} \Delta^{TH}}{\nu_{\max}}, \quad (5.13)$$

for suitable δ^{TH} and Δ^{TH} and for all $\hat{\mathbf{v}}_h \in \hat{V}_{h,0}^{TH}$ with $\mathbf{v}_h =: \hat{\mathbf{v}}_h \circ \mathbf{G}^{-1} \in V_{h,0}^{TH}$. In other words, we just need to prove the equivalence between $|\mathbf{v}_h|_{\mathbf{H}^1(\Omega)}$ and $|\hat{\mathbf{v}}_h|_{\mathbf{H}^1(\hat{\Omega})}$. One of the two bounds is

$$\begin{aligned} |\mathbf{v}_h|_{\mathbf{H}^1(\Omega)}^2 &= \int_{\Omega} \|\nabla \mathbf{v}_h\|_F^2 \, d\Omega = \int_{\hat{\Omega}} |\det(J_{\mathbf{G}})| \|\nabla \hat{\mathbf{v}}_h J_{\mathbf{G}}^{-1}\|_F^2 \, d\eta \\ &\leq \sup_{\hat{\Omega}} \left\{ |\det(J_{\mathbf{G}})| \|J_{\mathbf{G}}^{-1}\|_2^2 \right\} \int_{\hat{\Omega}} \|\nabla \hat{\mathbf{v}}_h\|_F^2 \, d\eta = \sup_{\hat{\Omega}} \left\{ |\det(J_{\mathbf{G}})| \|J_{\mathbf{G}}^{-1}\|_2^2 \right\} |\hat{\mathbf{v}}_h|_{\mathbf{H}^1(\hat{\Omega})}^2, \end{aligned} \quad (5.14)$$

where we used the fact that, given any two matrices X, Y with conforming dimensions, it holds $\|XY\|_F^2 \leq \|X\|_F^2 \|Y\|_2^2$. For the other bound, just observe that $\hat{\mathbf{v}}_h := \mathbf{v}_h \circ \mathbf{G}$, and then

$$|\hat{\mathbf{v}}_h|_{\mathbf{H}^1(\hat{\Omega})}^2 \leq \sup_{\hat{\Omega}} \left\{ |\det(J_{\mathbf{G}^{-1}})| \|J_{\mathbf{G}^{-1}}\|_2^2 \right\} |\mathbf{v}_h|_{\mathbf{H}^1(\Omega)}^2 = \sup_{\hat{\Omega}} \left\{ \frac{\|J_{\mathbf{G}}\|_2^2}{|\det(J_{\mathbf{G}})|} \right\} |\mathbf{v}_h|_{\mathbf{H}^1(\Omega)}^2; \quad (5.15)$$

This concludes the proof for the TH case.

The RT case is similar, we just highlight the differences. As above, from (5.10) and (5.11), we get

$$C_1 \|\mathbf{v}_h\|_{\mathbf{H}_{pen}^1(\Omega)}^2 \leq \mathbf{v}^T A^{RT} \mathbf{v} \leq C_2 \|\mathbf{v}_h\|_{\mathbf{H}_{pen}^1(\Omega)}^2, \quad (5.16)$$

$$\hat{C}_1 \|\hat{\mathbf{v}}_h\|_{\mathbf{H}_{pen}^1(\hat{\Omega})}^2 \leq \mathbf{v}^T P_V^{RT} \mathbf{v} \leq \hat{C}_2 \|\hat{\mathbf{v}}_h\|_{\mathbf{H}_{pen}^1(\hat{\Omega})}^2, \quad (5.17)$$

where $\hat{\mathbf{v}}_h \in \hat{V}_{h,0}^{RT}$, $\mathbf{v}_h = ((\det(J_{\mathbf{G}}))^{-1} J_{\mathbf{G}} \hat{\mathbf{v}}_h) \circ \mathbf{G}^{-1} = (\tilde{J}_{\mathbf{G}} \hat{\mathbf{v}}_h) \circ \mathbf{G}^{-1} \in V_{h,0}^{RT}$ and \mathbf{v} is the common coordinate vector. Then, we look for δ^{RT} and Δ^{RT} such that

$$\delta^{RT} \frac{\hat{C}_2}{C_1} \leq \frac{\|\mathbf{v}_h\|_{\mathbf{H}_{pen}^1(\Omega)}^2}{\|\hat{\mathbf{v}}_h\|_{\mathbf{H}_{pen}^1(\hat{\Omega})}^2} \leq \frac{\hat{C}_1}{C_2} \Delta^{RT}.$$

Direct computation shows that $\nabla(\tilde{J}_{\mathbf{G}} \hat{\mathbf{v}}_h) = \tilde{J}_{\mathbf{G}} \nabla \hat{\mathbf{v}}_h + \mathbb{H}_{\mathbf{G}} \hat{\mathbf{v}}_h$, where $\tilde{J}_{\mathbf{G}}$ and $\mathbb{H}_{\mathbf{G}}$ as in Section 3. It holds

$$\begin{aligned} |\mathbf{v}_h|_{\mathbf{H}^1(\Omega)}^2 &= \int_{\Omega} \|\nabla \mathbf{v}_h\|_F^2 \, d\Omega = \int_{\hat{\Omega}} |\det(J_{\mathbf{G}})| \left\| \nabla(\tilde{J}_{\mathbf{G}} \hat{\mathbf{v}}_h) J_{\mathbf{G}}^{-1} \right\|_F^2 \, d\hat{\Omega} \\ &\leq 2 \int_{\hat{\Omega}} |\det(J_{\mathbf{G}})| \left(\left\| \tilde{J}_{\mathbf{G}} \nabla \hat{\mathbf{v}}_h J_{\mathbf{G}}^{-1} \right\|_F^2 + \left\| (\mathbb{H}_{\mathbf{G}} \hat{\mathbf{v}}_h) J_{\mathbf{G}}^{-1} \right\|_F^2 \right) \, d\hat{\Omega} \\ &\leq 2 \sup_{\hat{\Omega}} \left\{ |\det(J_{\mathbf{G}})| \|J_{\mathbf{G}}^{-1}\|_2^2 \left\| \tilde{J}_{\mathbf{G}} \right\|_2^2, |\det(J_{\mathbf{G}})| \|J_{\mathbf{G}}^{-1}\|_2^2 \|\mathbb{H}_{\mathbf{G}}\|_F^2 \right\} \|\hat{\mathbf{v}}_h\|_{\mathbf{H}^1(\hat{\Omega})}^2, \end{aligned}$$

where $\|\mathbb{H}_{\mathbf{G}}\|_F^2$ is the Frobenius tensor norm of $\mathbb{H}_{\mathbf{G}}$. Moreover, it holds

$$\begin{aligned} \|\mathbf{v}_h\|_{L^2(\Omega)}^2 &= \int_{\Omega} |\mathbf{v}_h|^2 \, d\Omega = \int_{\hat{\Omega}} |\det(J_{\mathbf{G}})| \left\| \tilde{J}_{\mathbf{G}} \hat{\mathbf{v}}_h \right\|_2^2 \, d\hat{\Omega} \leq \sup_{\hat{\Omega}} \left\{ |\det(J_{\mathbf{G}})| \left\| \tilde{J}_{\mathbf{G}} \right\|_2^2 \right\} \|\hat{\mathbf{v}}_h\|_{L^2(\hat{\Omega})}^2, \\ \|\mathbf{v}_h\|_{L^2(\partial\Omega)}^2 &= \int_{\partial\Omega} |\mathbf{v}_h|^2 \, d\Gamma \leq \|\text{cof}(\nabla \mathbf{G})\|_{L^\infty(\hat{\Omega}),l} \int_{\partial\hat{\Omega}} \left\| \tilde{J}_{\mathbf{G}} \hat{\mathbf{v}}_h \right\|_2^2 \, d\hat{\Gamma} \\ &\leq \|\text{cof}(\nabla \mathbf{G})\|_{L^\infty(\hat{\Omega}),l} \sup_{\partial\hat{\Omega}} \left\{ \left\| \tilde{J}_{\mathbf{G}} \right\|_2^2 \right\} \|\hat{\mathbf{v}}_h\|_{L^2(\partial\hat{\Omega})}^2 \end{aligned}$$

where $\text{cof}(\cdot)$ refers to the matrix of the cofactors and $\|\cdot\|_{L^\infty(\widehat{\Omega}),l}$ is defined as in [42].

By observing that $\widehat{\mathbf{v}}_h = (\tilde{J}_{\mathbf{G}^{-1}} \mathbf{v}_h) \circ \mathbf{G}$, we can use similar argument to show that

$$\begin{aligned} \|\widehat{\mathbf{v}}_h\|_{\mathbf{H}^1(\widehat{\Omega})}^2 &\leq 2 \sup_{\Omega} \left\{ |\det(J_{\mathbf{G}^{-1}})| \|J_{\mathbf{G}^{-1}}^{-1}\|_2^2 \|\tilde{J}_{\mathbf{G}^{-1}}\|_2^2, |\det(J_{\mathbf{G}^{-1}})| \|J_{\mathbf{G}^{-1}}^{-1}\|_2^2 \|\mathbb{H}_{\mathbf{G}^{-1}}\|_F^2 \right\} \|\mathbf{v}_h\|_{\mathbf{H}^1(\Omega)}^2, \\ \|\widehat{\mathbf{v}}_h\|_{L^2(\widehat{\Omega})}^2 &\leq \sup_{\Omega} \left\{ |\det(J_{\mathbf{G}^{-1}})| \|\tilde{J}_{\mathbf{G}^{-1}}\|_2^2 \right\} \|\mathbf{v}_h\|_{L^2(\Omega)}^2, \\ \|\widehat{\mathbf{v}}_h\|_{L^2(\partial\widehat{\Omega})}^2 &\leq \|\text{cof}(\nabla \mathbf{G}^{-1})\|_{L^\infty(\Omega),l} \sup_{\partial\Omega} \left\{ \|\tilde{J}_{\mathbf{G}^{-1}}\|_2^2 \right\} \|\mathbf{v}_h\|_{L^2(\partial\Omega)}^2. \end{aligned}$$

This concludes the analysis of the RT case. □

We next analyse $P_Q^{-1}Q$.

Theorem 2. *It holds*

$$\theta \geq \lambda_{\min}(P_Q^{-1}Q), \quad \lambda_{\max}(P_Q^{-1}Q) \leq \Theta, \quad (5.18)$$

where θ and Θ are positive constants that do not depend on h or on p .

Proof. We report the proof for TH discretization. The proof for the RT discretization can be derived in a analogous way.

By Courant-Fischer theorem, we need to prove

$$\theta \leq \frac{\langle Q\mathbf{g}, \mathbf{g} \rangle}{\langle P_Q\mathbf{g}, \mathbf{g} \rangle} \leq \Theta \quad \forall \mathbf{g} \in \mathbb{R}^{n_Q}.$$

Let $\mathbf{g} \in \mathbb{R}^{n_Q}$ and $g_h = \sum_{i=1}^{n_Q} [\mathbf{g}]_i \hat{B}_{\alpha,i}^p$. It holds

$$\mathbf{g}^T Q^{TH} \mathbf{g} = \int_{\widehat{\Omega}} g_h^2 \nu^{-1} |\det(J_{\mathbf{G}})| \, d\widehat{\Omega} \leq \sup_{\widehat{\Omega}} (|\det(J_{\mathbf{G}})| \nu^{-1}) \int_{\widehat{\Omega}} g_h^2 \, d\widehat{\Omega} \leq \sup_{\widehat{\Omega}} (|\det(J_{\mathbf{G}})| \nu^{-1}) \mathbf{g}^T P_Q^{TH} \mathbf{g}, \quad (5.19)$$

and, in an analogous way, one can prove the other side of the inequality. □

Remark 1. *The constants δ , Δ , θ and Θ depend on the parametrization \mathbf{G} and on the kinematic viscosity ν . This dependence can be inferred from the proof of Theorems 1–2. Considering for example the TH case, from (5.13)–(5.15) and using*

$$\left[\sup_{\widehat{\Omega}} \left\{ \frac{\|J_{\mathbf{G}}\|_2^2}{|\det(J_{\mathbf{G}})|} \right\} \right]^{-1} = \inf_{\widehat{\Omega}} \left\{ \frac{|\det(J_{\mathbf{G}})|}{\|J_{\mathbf{G}}\|_2^2} \right\},$$

we get to the following admissible choices

$$\delta^{TH} = C_{\text{Korn}} \nu_{\min} \inf_{\widehat{\Omega}} \left\{ \frac{|\det(J_{\mathbf{G}})|}{\|J_{\mathbf{G}}\|_2^2} \right\} \quad \text{and} \quad \Delta^{TH} = \hat{C}_{\text{Korn}}^{-1} \nu_{\max} \sup_{\widehat{\Omega}} \left\{ |\det(J_{\mathbf{G}})| \|J_{\mathbf{G}}\|_2^2 \right\}.$$

In a similar way, from (5.19), we have following admissible choices

$$\theta^{TH} = \inf_{\widehat{\Omega}} (|\det(J_{\mathbf{G}})| \nu^{-1}), \quad \text{and} \quad \Theta^{TH} = \sup_{\widehat{\Omega}} (|\det(J_{\mathbf{G}})| \nu^{-1}).$$

5.2 Preconditioners application: FD method

At each iteration of our iterative solver we have to solve

$$\mathcal{P}s = r, \quad (5.20)$$

where r is the current residual and \mathcal{P} is a preconditioner, that can be either matrix from (4.2), (4.3) and (4.4). Besides multiplications by B or B^T , to accomplish this task we need to solve the linear systems with matrices P_V and P_Q . Thanks to (2.15) and the band structure of the univariate factors in (5.7), the solution of a linear system with matrix P_Q is obtained in a direct way with only $O(pn_Q)$ FLOPs.

On the other hand, the solution of a linear system with matrix P_V requires to solve three Sylvester-like equations, one for each diagonal block $P_{V,k}$. Following [20], to accomplish this aim we use the Fast Diagonalization (FD) direct method of [29] and [28]. We now briefly explain its main features.

Consider the general Sylvester-like system:

$$Rq := (K_3 \otimes M_2 \otimes M_1 + M_3 \otimes K_2 \otimes M_1 + M_3 \otimes M_2 \otimes K_1) q = t, \quad (5.21)$$

with both M_i and K_i symmetric and positive definite matrices for $i = 1, 2, 3$. Let

$$K_i U_i = M_i U_i D_i, \quad i = 1, 2, 3, \quad (5.22)$$

be the eigendecomposition of the pencils (K_i, M_i) , where D_i are diagonal matrices containing the eigenvalues of $M_i^{-1} K_i$ and $U_i^T M_i U_i = I$. We have $M_i = U_i^{-T} U_i^{-1}$ and $K_i = U_i^{-T} D_i U_i^{-1}$. Then, we can factorize R as

$$R = (U_3 \otimes U_2 \otimes U_1)^{-T} (I \otimes I \otimes D_1 + I \otimes D_2 \otimes I + D_3 \otimes I \otimes I) (U_3 \otimes U_2 \otimes U_1)^{-1}.$$

Exploiting (2.12), (2.14) and the factorization above, the solution of (5.21) can be computed by the following algorithm.

Algorithm 1 3D FD method

- 1: Compute the generalized eigendecompositions (5.22)
 - 2: Compute $\tilde{t} = (U_1 \otimes U_2 \otimes U_3)^T t$
 - 3: Compute $\tilde{q} = (I \otimes I \otimes D_1 + I \otimes D_2 \otimes I + D_3 \otimes I \otimes I)^{-1} \tilde{t}$
 - 4: Compute $q = (U_1 \otimes U_2 \otimes U_3) \tilde{q}$
-

Assuming for simplicity that the matrices K_i and M_i all have the same order n , Algorithm 1 requires $12n^4 + O(n^3) = 12n_{dof}^{4/3} + O(n_{dof})$ FLOPs, where $n_{dof} = n^3$ denotes the order of R . Step 1 and step 3 are optimal as they require only $O(n_{dof})$ FLOPs. The asymptotic dominant cost, i.e. $12n_{dof}^{4/3}$ FLOPs, is related to the matrix-matrix products of step 2 and step 4, while step 1 and step 3 are optimal as they require only $O(n_{dof})$ FLOPs. However step 2 and step 4, being BLAS level 3 operations, are typically implemented in a highly efficient way on modern computers. As a consequence, despite their superlinear computational cost, in practice they do not dominate the computational time of the overall iterative strategy (see the numerical experiments of [20] and the ones in the present paper for more details on this important point).

6 Preconditioners for P_V and P_Q including coefficients information

The proposed preconditioners P_V and P_Q from Section 5 are robust with respect to the mesh size and spline degree. However they do not incorporate any information from the coefficients (either the geometry map \mathbf{G}

and or the kinematic viscosity ν) and in fact the preconditioner's quality is affected from the coefficients. This is reflected in the analysis of Section 5.1 (see Remark 1 for the TH case). Numerical tests of Section 7 confirm this expectation. We therefore present two strategies that partially incorporate ν and \mathbf{G} in P_V and P_Q , without increasing the preconditioners computational cost.

First, we consider a diagonal scaling. In particular, we replace P_Q by $P_Q^{\mathbf{G}} := D_Q^{1/2} P_Q D_Q^{1/2}$, where D_Q is a diagonal matrices having diagonal entries $[D_Q]_{i,i} = [Q]_{i,i} / [P_Q]_{i,i}$. Even though we postpone a mathematical analysis of it to a further work, the numerical tests in Section 7 show that this cheap modification of the preconditioner is sufficient to give $P_Q^{\mathbf{G}}$ robustness with respect to the coefficients (not only \mathbf{G} , as indicated, but also ν).

The same idea, applied to P_V , while able to incorporate efficiently the contribution of the scalar coefficient ν , is less effective when the geometry parametrization is far from a scaled identity. In this case we propose to incorporate some components of the geometry parametrization into the univariate matrix factors appearing in (5.4) and (5.5) (see the Appendix for details) in order to build a preconditioner \widehat{P}_V such that Algorithm 1 can still be used. Then, we apply a diagonal scaling. This leads to an effective preconditioner having the form $P_V^{\mathbf{G}} := D_V^{1/2} \widehat{P}_V D_V^{1/2}$, where D_V has diagonal entries $[D_V]_{i,i} = [A]_{i,i} / [\widehat{P}_V]_{i,i}$.

We use the following notation: $\mathcal{P}_D^{\mathbf{G}}$, $\mathcal{P}_T^{\mathbf{G}}$ and $\mathcal{P}_C^{\mathbf{G}}$ are the preconditioner matrices for the Stokes system obtained by replacing P_V and P_Q with $P_V^{\mathbf{G}}$ and $P_Q^{\mathbf{G}}$ in (4.2), (4.3) and (4.4), respectively. The corresponding preconditioned strategies are then referred to as $\mathcal{P}_D^{\mathbf{G}}$ -MINRES, $\mathcal{P}_T^{\mathbf{G}}$ -GMRES and $\mathcal{P}_C^{\mathbf{G}}$ -GMRES.

7 Numerical results

We present here numerical experiments to show the performance of our preconditioning strategies. All the tests are performed by Matlab (version 8.5.0.197613 R2015a) and using the GeoPDEs toolbox [43], on a Intel Xeon i7-5820K processor, running at 3.30 GHz, and with 64 GB of RAM. We restrict our tests to a single computational thread. Indeed, even though our strategy would likely benefit from parallelization on a multicore hardware, as its main computational efforts are matrix products, a careful analysis of the parallel implementation would require an in-depth study, which is beyond the scope of this work.

In the construction and application of our preconditioner the two dominant steps are the eigendecomposition of the univariate matrices (step 1 in Algorithm 1) and the multiplication of Kronecker matrices (steps 2 and 4 in Algorithm 1). These two key operations are performed by the `eig` Matlab function and by the Tensorlab toolbox [44], respectively. The partial inclusion of the geometry has a negligible cost (see the Appendix). The tolerance of both MINRES and GMRES is set to 10^{-8} and the initial guess is the null vector in all tests.

As a comparison, we consider a block-diagonal preconditioner based on an incomplete Cholesky factorization. In our case, the zero-fill incomplete Cholesky factorization, denoted IC(0), is computed by the MATLAB `ichol` routine for the matrix

$$\begin{bmatrix} A_{11} & 0 & 0 & 0 \\ 0 & A_{22} & 0 & 0 \\ 0 & 0 & A_{33} & 0 \\ 0 & 0 & 0 & Q \end{bmatrix}$$

and then used in a Conjugate Gradient (CG) inner iteration in order to approximate the application of the

ideal preconditioner

$$\begin{bmatrix} A_{11} & A_{12} & A_{13} & 0 \\ A_{21} & A_{22} & A_{23} & 0 \\ A_{31} & A_{32} & A_{33} & 0 \\ 0 & 0 & 0 & Q \end{bmatrix}. \quad (7.1)$$

This strategy is denoted IC(0)-MINRES. The tolerance of this inner CG loop is set to 10^{-2} as this maximizes the efficiency of the overall strategy in the numerical tests we consider below. The inner loop is needed to achieve robustness with respect to h , while robustness with respect to p is common for incomplete factorizations. For this reason, incomplete factorizations are often adopted in IGA as preconditioners: in the context of the Stokes system, see [21] where a similar approach is considered and benchmarked.

We remark that the geometry parametrization, without simplifications, is directly incorporated in the preconditioner (7.1). Therefore, as it is seen in the tests below, IC(0)-MINRES behaves quite robustly with respect to the geometry parametrizations (since $\lambda_{\max}(Q^{-1}BA^{-1}B^T)$ and $\lambda_{\min}(Q^{-1}BA^{-1}B^T)$ depend on Ω , some dependence on the shape of the domain is unavoidable), while the geometry parametrization has a critical role in our strategies. Also for this reason, IC(0)-MINRES is an important term of comparison.

We consider three different geometries, with increasing complexity (from the point of view of the geometry parametrization): the cube, the eighth of annulus, and a hollow torus with an eccentric annular cross-section (see Figure 1).

As discussed in Section 3, the Stokes problem is discretized using the spaces $V_{h,0}^{TH}$, $Q_{h,0}^{TH}$, $V_{h,0}^{RT}$ and $Q_{h,0}^{RT}$ defined respectively in (2.6a), (2.7), (2.10a) and (2.11). In all our tests we choose a uniform regularity $\alpha = (\alpha, \alpha, \alpha)$ with $\alpha = p - 1$, except for the hollow torus domain where the spaces are C^0 at the boundary of the initial mesh elements, and C^α , $\alpha = p - 1$, once the mesh is refined. Note that p always refers to the spline degree of the pressure space. For Raviart-Thomas discretizations we choose $C_{pen} = 5(\alpha + 1)$ in (3.5), as it numerically leads to stable schemes (see [12]).

Tables 1–10 report the total solving time, which includes the preconditioner setup and the MINRES/GMRES iterations. However, we exclude the time for the formation of the pressure mass matrix Q , which is needed in IC(0) and \mathcal{P}_D^G , \mathcal{P}_T^G , \mathcal{P}_C^G setup (though only the main diagonal of Q is needed in our approaches, and, in all cases, only a low-order approximation of Q is needed for preconditioning). Indeed, it is well known that the formation of isogeometric matrices is expensive unless ad-hoc routines are adopted (e.g. the weighted-quadrature approach [45] or the low-rank approach [46]). In this paper, we only focus on the solver and do not address the efficient formation of the matrix. We denote by n_{el} the number of elements in each parametric direction. The symbol “*” denotes the impossibility of formation of the matrix \mathcal{A} , due to memory requirements.

In Table 7 we report, only for the eighth of annulus testcase, the preconditioner setup time and the preconditioner application time, separately, and in Table 8 we report the percentage of computing time spent in the preconditioner application. Finally, Table 11 contains number of iterations and solving times obtained with three different choices of variable kinematic viscosity ν in the hollow torus domain.

Cube We first consider the symmetric driven cavity problem in $\Omega = \widehat{\Omega} = [0, 1]^3$ (Figure 1a). In this case, \mathbf{G} is the identity map and therefore $A_{kk} = P_{V,k}$. Homogeneous boundary conditions for the velocity on the lateral sides of the cube and a velocity equal to $[1, 0, 0]^T$ at the top and to $[-1, 0, 0]^T$ at the bottom are imposed, while f is the null function and $\nu = 1$.

In Table 1 we report, for the TH discretization, \mathcal{P}_D -MINRES and IC(0)-MINRES performances. The former is much faster, especially for high degree. \mathcal{P}_D -MINRES results with RT discretization are reported in Table 2. The computational time is lower compared to TH discretization since, for equal mesh sizes, the TH

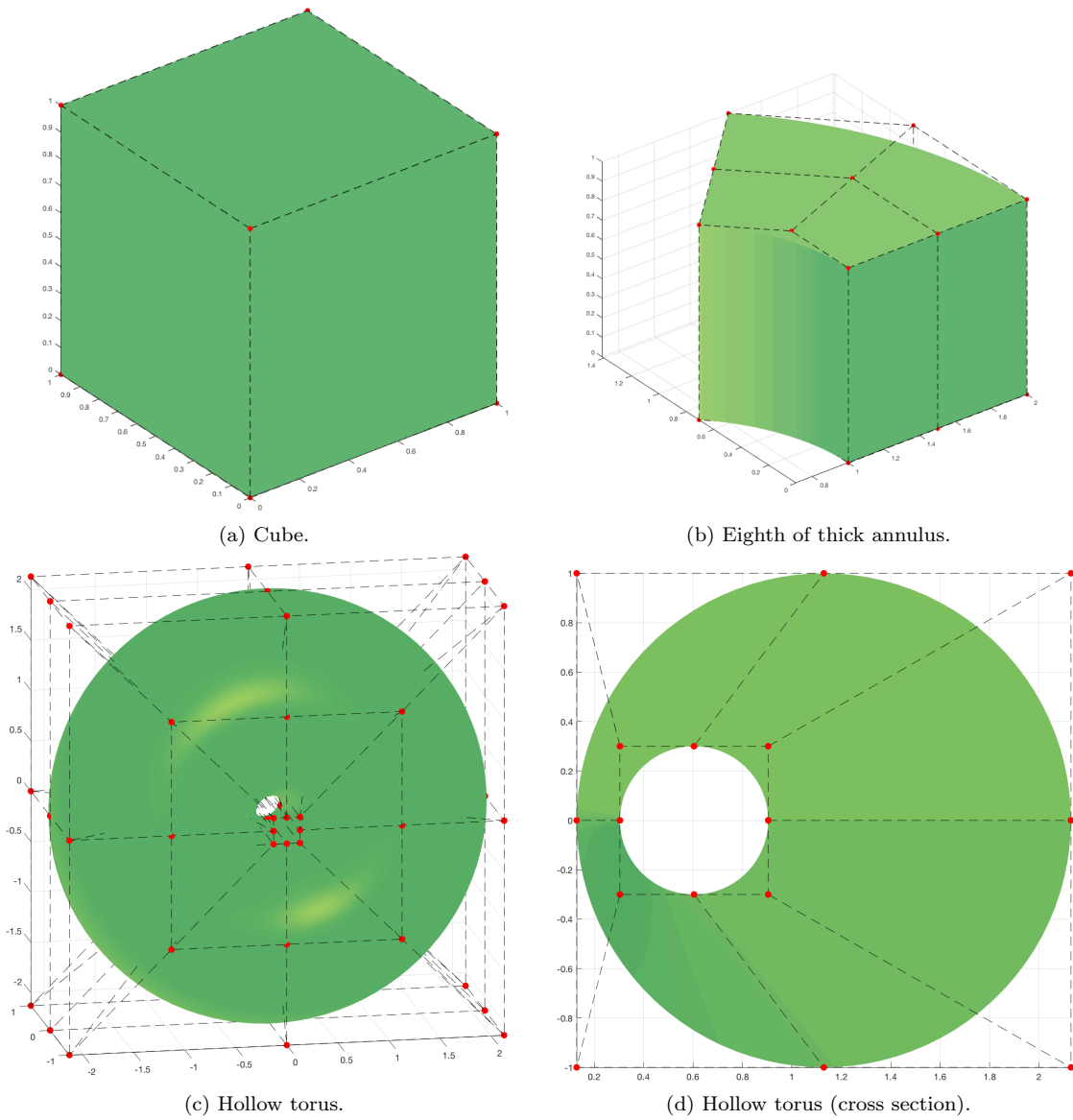


Figure 1: Computational domains.

	(TH) \mathcal{P}_D -MINRES		Iterations / Time (sec)	
n_{el}	$p = 2$	$p = 3$	$p = 4$	$p = 5$
4	48 / 0.16	51 / 0.21	52 / 0.43	52 / 0.81
8	53 / 0.74	53 / 1.49	53 / 3.01	53 / 5.70
16	56 / 5.61	56 / 12.76	56 / 26.54	56 / 51.00
32	56 / 52.23	56 / 114.07	*	*

	(TH) IC(0)-MINRES		Iterations / Time (sec)	
n_{el}	$p = 2$	$p = 3$	$p = 4$	$p = 5$
4	35 / 0.22	37 / 0.69	37 / 1.71	37 / 3.77
8	34 / 2.82	37 / 7.22	35 / 16.10	36 / 33.76
16	35 / 35.09	35 / 74.34	35 / 151.87	35 / 305.90
32	36 / 482.25	36 / 902.51	*	*

Table 1: Cube domain (TH). Performance of \mathcal{P}_D -MINRES (upper table) and IC(0)-MINRES (lower table).

	(RT) \mathcal{P}_D -MINRES		Iterations / Time (sec)	
n_{el}	$p = 2$	$p = 3$	$p = 4$	$p = 5$
4	43 / 0.13	46 / 0.18	48 / 0.23	48 / 0.39
8	54 / 0.23	52 / 0.44	52 / 0.85	52 / 1.59
16	55 / 0.95	53 / 2.56	52 / 4.77	52 / 9.02
32	55 / 6.39	54 / 16.67	52 / 34.58	*

Table 2: Cube domain (RT). Performance of \mathcal{P}_D -MINRES.

velocity space is about 2^3 times bigger than the one for RT. In all cases the number of iterations is uniformly bounded with respect to p and n_{el} .

Eighth of thick annulus Now we consider the eighth of a thick annulus domain (Figure 1b). The internal radius and the height are equal to 1, while the external radius is equal to 2. The boundary data represent a generalization of the symmetric driven cavity boundary conditions, i.e. the velocity is constrained to be $[-1, 0, 0]^T$ on the set $\{y = 0\}$ and $[\sqrt{2}/2, \sqrt{2}/2, 0]^T$ on the opposite side, while homogeneous boundary conditions are imposed anywhere else. Note that in this case $A_{kk} \neq P_{V,k}$. The kinematic viscosity ν is constant and equal to 1.

Table 3 shows the results of \mathcal{P}_D -MINRES, \mathcal{P}_D^G -MINRES and IC(0)-MINRES for TH discretization. Again, IC(0)-MINRES is not competitive with \mathcal{P}_D -MINRES and \mathcal{P}_D^G -MINRES in terms of computing time. The use of \mathcal{P}_D^G -MINRES halves the number of iterations and the solving time w.r.t. \mathcal{P}_D -MINRES, indicating that the inclusion of some geometry information improves the performance of the preconditioner. In Table (4) we report results for \mathcal{P}_D^G -MINRES with RT discretization. The performances of \mathcal{P}_T^G -GMRES and \mathcal{P}_C^G -GMRES with TH and RT discretizations are reported in Table 5 and Table 6 respectively. We do not report results for \mathcal{P}_T -GMRES and \mathcal{P}_C -GMRES, as the effect of not including any geometry in the preconditioners is similar to the case of the block diagonal preconditioner. We see that, though the number of iterations of both \mathcal{P}_T^G -GMRES and \mathcal{P}_C^G -GMRES is lower than \mathcal{P}_D^G -MINRES, they are comparable to it in terms of

CPU time. This is due the higher application cost of the block triangular and constraint preconditioners (which is mainly related to the matrix-vector products with B and B^T). We emphasize that, again, in all the FD-based strategies the number of iterations is uniformly bounded with respect to p and n_{el} .

In order to better understand the behaviour of the preconditioners, and identify directions of further improvements, we analyse in Table 7 the computational costs for the setup and the application of the preconditioners. We recall that for IC(0)-MINRES, the application corresponds to the execution of the inner CG iterative solver with residual tolerance 10^{-2} . In all cases, we assume the pressure mass matrix Q is given. Table 7 reports the total time spent in the preconditioner setup and application. We clearly see that the FD-based preconditioners are much faster than the incomplete factorization. Note that the setup time for \mathcal{P}_D^G is higher than for \mathcal{P}_D due to the cost of computing the separable approximation of the geometry (see the Appendix): further studies and tune up of this procedure will be considered in our following works.

In Table 8, preconditioner application time is compared with the overall computation time of the iterative solver. With \mathcal{P}_D^G -MINRES strategy, the percentage of time spent for the preconditioner is negligible, e.g. when $p = 5$ and $n_{el} = 16$ it is less than 1%. The computation time is indeed mainly spent in the matrix-vector multiplication. This situation suggests that further improvements could be obtained shifting towards a matrix-free implementation [30].

The results of Table 7 and 8 clearly show that the suboptimal asymptotic cost $O(n_{dof}^{4/3})$ of the preconditioner is not seen in practice, up to the largest problem tested. Note in particular from Table 7 that the application times of the FD-based preconditioners scale with respect to h much better than the asymptotic cost would suggest. This is due to the high efficiency of the routines that computes the dense matrix-matrix products that are the core of the FD method.

Hollow torus The last domain examined is a torus with a hole (Figure 1c), obtained by revolving an eccentric annulus (Figure 1d) around the y axis. We take $f = [\cos(\arctan(x/z)), \sin(4\pi x), \sin(\arctan(x/z))]^T$, $\nu = 1$ and we impose homogeneous Dirichlet boundary conditions anywhere on the external boundary. We consider here the periodic setting, imposing C^0 periodic continuity in the function space. For this problem, we present only TH discretization results and focus on the effects of the geometry parametrization on the performances of the preconditioning strategies. Computing time and number of iterations of \mathcal{P}_D -MINRES, \mathcal{P}_D^G -MINRES and IC(0)-MINRES are reported in Table 9. As expected, the geometry parametrization of the hollow torus has a non-negligible influence on the performance of our preconditioners.

This is especially true for the \mathcal{P}_D -MINRES strategy, that requires thousands of iterations to converge. On the other hand, this influence is greatly reduced with partial inclusion of the geometry (\mathcal{P}_D^G -MINRES). Here the number of iterations and the CPU times are two orders of magnitude lower than for \mathcal{P}_D -MINRES. CPU times for \mathcal{P}_D^G -MINRES are also significantly better than for IC(0)-MINRES, despite the fact the number of iterations is higher. Finally, we remark that the number of iterations for \mathcal{P}_D^G -MINRES is only three times higher than \mathcal{P}_D -MINRES on the cube.

Hollow torus: variable ν In this paragraph we investigate the effect of a variable kinematic viscosity ν on our preconditioning strategies. We consider the hollow torus domain with $\nu = 1 + (k - 1)(1 + \cos(\arctan(x/z)))/2$ depending on a parameter k , $p = 3$ and $n_{el} = 32$ and we compare in Table 11 the performances of \mathcal{P}_D -MINRES, \mathcal{P}_D^G -MINRES and \mathcal{P}_T^G -GMRES.

\mathcal{P}_D -MINRES is the worse strategy both in terms of number of iterations and in computing times for all values of k and in the case $k = 10000$ it does not even converge. The geometry inclusion strategy, on the other hand, succeeds in capturing the effect of the variable ν ; the number of iterations of \mathcal{P}_D^G -MINRES and \mathcal{P}_T^G -GMRES remains stable when k varies.

	(TH) \mathcal{P}_D -MINRES		Iterations / Time (sec)	
n_{el}	$p = 2$	$p = 3$	$p = 4$	$p = 5$
4	116 / 0.39	128 / 0.56	137 / 1.12	146 / 2.14
8	146 / 1.66	153 / 4.02	158 / 8.79	160 / 16.83
16	163 / 16.53	164 / 38.54	165 / 75.95	162 / 138.17
32	169 / 181.68	166 / 337.37	*	*

	(TH) \mathcal{P}_D^G -MINRES		Iterations / Time (sec)	
n_{el}	$p = 2$	$p = 3$	$p = 4$	$p = 5$
4	65 / 0.21	68 / 0.33	69 / 0.57	72 / 1.09
8	72 / 0.91	74 / 2.06	74 / 4.24	75 / 8.01
16	77 / 8.11	77 / 18.82	77 / 36.70	77 / 67.74
32	79 / 90.56	79 / 168.60	*	*

	(TH) IC(0)-MINRES		Iterations / Time (sec)	
n_{el}	$p = 2$	$p = 3$	$p = 4$	$p = 5$
4	39 / 0.28	39 / 0.79	41 / 1.64	41 / 32.69
8	39 / 3.13	39 / 7.44	39 / 16.47	39 / 32.69
16	40 / 39.44	39 / 80.53	37 / 157.37	37 / 281.24
32	38 / 611.55	38 / 1085.21	*	*

Table 3: Eighth of thick annulus domain (TH). Performance of \mathcal{P}_D -MINRES (upper table), \mathcal{P}_D^G -MINRES (middle table) and IC(0)-MINRES (lower table).

	(RT) \mathcal{P}_D^G -MINRES		Iterations / Time (sec)	
n_{el}	$p = 2$	$p = 3$	$p = 4$	$p = 5$
4	59 / 0.22	58 / 0.17	62 / 0.30	63 / 0.54
8	63 / 0.29	63 / 0.58	61 / 1.09	64 / 2.10
16	67 / 1.36	65 / 3.23	65 / 6.37	66 / 12.07
32	65 / 8.71	66 / 23.73	66 / 48.38	*

Table 4: Eighth of thick annulus domain (RT). Performance of \mathcal{P}_D^G -MINRES.

	(TH) \mathcal{P}_T^G -GMRES		Iterations / Time (sec)	
n_{el}	$p = 2$	$p = 3$	$p = 4$	$p = 5$
4	38 / 0.20	42 / 0.28	42 / 0.56	47 / 1.17
8	41 / 0.78	42 / 1.78	43 / 4.50	45 / 8.50
16	43 / 7.57	44 / 17.52	45 / 35.43	46 / 66.21
32	45 / 76.69	46 / 165.72	*	*

	(TH) \mathcal{P}_C^G -GMRES		Iterations / Time (sec)	
n_{el}	$p = 2$	$p = 3$	$p = 4$	$p = 5$
4	35 / 0.21	37 / 0.30	39 / 0.59	41 / 1.15
8	37 / 0.80	38 / 1.77	39 / 4.33	41 / 8.25
16	38 / 7.19	39 / 16.51	40 / 33.47	41 / 62.98
32	39 / 61.29	40 / 152.44	*	*

Table 5: Eighth of thick annulus domain (TH). Performance of \mathcal{P}_T^G -GMRES (upper table) and \mathcal{P}_C^G -GMRES (lower table).

	(RT) \mathcal{P}_T^G -GMRES		Iterations / Time (sec)	
n_{el}	$p = 2$	$p = 3$	$p = 4$	$p = 5$
4	41 / 0.19	44 / 0.20	46 / 0.35	48 / 0.69
8	46 / 0.34	47 / 0.71	49 / 1.48	50 / 5.55
16	47 / 1.72	49 / 7.77	50 / 16.57	52 / 32.86
32	48 / 21.15	50 / 56.50	52 / 120.06	*

	(RT) \mathcal{P}_C^G -GMRES		Iterations / Time (sec)	
n_{el}	$p = 2$	$p = 3$	$p = 4$	$p = 5$
4	37 / 0.19	38 / 0.22	39 / 0.36	40 / 0.68
8	38 / 0.34	40 / 0.71	41 / 1.41	42 / 4.98
16	39 / 1.63	40 / 6.81	41 / 14.42	42 / 28.18
32	39 / 18.30	40 / 48.05	41 / 100.99	*

Table 6: Eighth of thick annulus domain (RT). Performance of \mathcal{P}_T^G -GMRES (upper table) and \mathcal{P}_C^G -GMRES (lower table).

\mathcal{P}_D Setup times / Total Application times (\mathcal{P}_D -MINRES)				
n_{el}	$p = 2$	$p = 3$	$p = 4$	$p = 5$
4	0.02 / 0.19	0.02 / 0.20	0.02 / 0.20	0.03 / 0.21
8	0.04 / 0.27	0.04 / 0.29	0.04 / 0.33	0.04 / 0.37
16	0.05 / 0.87	0.06 / 0.95	0.06 / 1.09	0.06 / 1.18
32	0.09 / 7.21	0.12 / 9.94	*	*

\mathcal{P}_D^G Setup times / Total Application times (\mathcal{P}_D^G -MINRES)				
n_{el}	$p = 2$	$p = 3$	$p = 4$	$p = 5$
4	0.05 / 0.88	0.06 / 0.10	0.06 / 0.10	0.07 / 0.11
8	0.09 / 0.13	0.12 / 1.49	0.16 / 0.16	0.21 / 0.18
16	0.28 / 0.46	0.49 / 0.51	0.76 / 0.56	1.14 / 0.62
32	1.57 / 3.86	3.20 / 3.93	*	*

IC(0) Setup times / Total Application times (IC(0)-MINRES)				
n_{el}	$p = 2$	$p = 3$	$p = 4$	$p = 5$
4	0.01 / 0.21	0.03 / 0.59	0.12 / 1.43	0.38 / 3.04
8	0.09 / 2.55	0.45 / 6.02	1.46 / 13.05	4.23 / 23.98
16	0.94 / 34.49	4.36 / 66.68	13.90 / 125.35	40.91 / 207.12
32	9.09 / 558.27	46.65 / 889.03	*	*

Table 7: Eight of thick annulus domain (TH). Setup times and total application times of the preconditioners \mathcal{P}_D (top table), \mathcal{P}_D^G (middle table) and IC(0) (bottom table).

\mathcal{P}_D^G				
n_{el}	$p = 2$	$p = 3$	$p = 4$	$p = 5$
8	14.28%	6.79%	3.77%	2.24%
16	5.67%	2.70%	1.52%	0.91%
32	4.26 %	2.33%	*	*

IC(0)				
n_{el}	$p = 2$	$p = 3$	$p = 4$	$p = 5$
8	81.46%	80.91%	79.23%	73.35%
16	87.44%	82.80%	79.65%	73.64%
32	91.28%	81.92%	*	*

Table 8: Eight of thick annulus domain (TH). Percentage of computing time of the preconditioner application in each MINRES iteration: \mathcal{P}_D^G (top table) and IC(0) (bottom table).

	(TH) \mathcal{P}_D -MINRES Iterations / Time (sec)			
n_{el}	$p = 2$	$p = 3$	$p = 4$	$p = 5$
4	2004 / 6.42	4125 / 39.16	6411 / 153.95	8305 / 478.69
8	5524 / 80.73	7875 / 360.15	9914 / 1117.12	11032 / 3286.67
16	9931 / 1081.01	11780 / 3763.90	12964 / 8776.73	13553 / 18626.03
32	12864 / 10244.45	13426 / 29344.81	*	*

	(TH) \mathcal{P}_D^G -MINRES Iterations / Time (sec)			
n_{el}	$p = 2$	$p = 3$	$p = 4$	$p = 5$
4	77 / 0.31	87 / 0.89	97 / 2.59	104 / 6.24
8	96 / 1.52	104 / 4.99	110 / 12.82	115 / 34.70
16	119 / 13.87	124 / 40.89	133 / 91.82	139 / 197.30
32	142 / 116.95	147 / 344.34	*	*

	(TH) IC(0)-MINRES Iterations / Time (sec)			
n_{el}	$p = 2$	$p = 3$	$p = 4$	$p = 5$
4	49 / 1.05	46 / 3.74	50 / 11.79	50 / 31.42
8	45 / 5.42	45 / 18.52	45 / 51.18	45 / 126.83
16	45 / 45.11	43 / 125.60	45 / 307.79	45 / 660.63
32	45 / 493.12	44 / 1352.81	*	*

Table 9: Hollow torus domain (TH). Performance of \mathcal{P}_D -MINRES (upper table), \mathcal{P}_D^G -MINRES (middle table) and IC(0)-MINRES (lower table).

	(TH) \mathcal{P}_T^G -GMRES Iterations / Time (sec)			
n_{el}	$p = 2$	$p = 3$	$p = 4$	$p = 5$
4	44 / 0.30	50 / 0.80	57 / 2.39	61 / 6.89
8	49 / 1.25	54 / 4.54	58 / 11.98	62 / 31.52
16	58 / 10.78	60 / 32.86	63 / 73.52	67 / 159.46
32	68 / 105.31	71 / 275.54	*	*

	(TH) \mathcal{P}_C^G -GMRES Iterations / Time (sec)			
n_{el}	$p = 2$	$p = 3$	$p = 4$	$p = 5$
4	37 / 0.28	41 / 0.74	45 / 2.09	50 / 6.09
8	41 / 1.16	45 / 4.07	49 / 10.82	53 / 28.59
16	51 / 10.27	55 / 31.73	59 / 72.91	63 / 158.12
32	69 / 113.81	72 / 299.62	*	*

Table 10: Hollow torus domain (TH). Performance of \mathcal{P}_T^G -GMRES (upper table) and \mathcal{P}_C^G -GMRES (lower table)

	\mathcal{P}_D -MINRES	$\mathcal{P}_D^{\mathcal{G}}$ -MINRES	$\mathcal{P}_T^{\mathcal{G}}$ -GMRES
$k = 1$	13426 / 29344.81	147 / 344.34	71 / 275.54
$k = 100$	17254 / 37667.04	180 / 400.46	84 / 325.02
$k = 10000$	–	180 / 407.68	84 / 326.78

Table 11: Hollow torus domain (TH). Performance of \mathcal{P}_D -MINRES, $\mathcal{P}_D^{\mathcal{G}}$ -MINRES and $\mathcal{P}_T^{\mathcal{G}}$ -GMRES for $p = 3$ and $n_{el} = 32$. The symbol “–” denotes the fact the the solver does not converge because of stagnation.

We remark that $\mathcal{P}_C^{\mathcal{G}}$ -GMRES has behaviour similar to $\mathcal{P}_T^{\mathcal{G}}$ -GMRES, as it is also highlighted in the previous testcases, and for this reason we do not consider it in the table.

8 Conclusions

In this work we have addressed the problem of finding good preconditioners for isogeometric discretizations of the Stokes system. Our approach exploits the tensor-product structure of the multivariate B-spline basis. The application of our preconditioners \mathcal{P}_D , \mathcal{P}_T and \mathcal{P}_C (and their coefficients-including variants $\mathcal{P}_D^{\mathcal{G}}$, $\mathcal{P}_T^{\mathcal{G}}$ and $\mathcal{P}_C^{\mathcal{G}}$) requires the solution of linear systems that have a Kronecker structure, or a Sylvester-like equation structure. This can be performed by direct solvers with the highest efficiency. This also guarantees robustness with respect to both the spline degree p and mesh resolution. Numerical tests show that $\mathcal{P}_D^{\mathcal{G}}$, $\mathcal{P}_T^{\mathcal{G}}$ and $\mathcal{P}_C^{\mathcal{G}}$ allow to maintain the performance also in case of non-trivial geometries and highly oscillating coefficients.

We have performed a comparative numerical benchmarking with respect to a more common approach which uses a similar block structure for the preconditioner but applies it by an incomplete Cholesky factorization and an inner conjugate gradient. The solution time is always in favour of our preconditioners, despite that they are influenced by the geometry parametrization. Even more important is that our preconditioners are well suited for a matrix-free approach, which should lead to solvers that are orders of magnitude faster. This is the most promising research direction that we will consider in the near future [30].

There are other important extensions to this work that will be the topic of our future researches. Multipatch geometries are possible by combining our framework to known domain decomposition techniques, e.g. FETI-DP [23]. A challenging extension is to the Oseen system, in particular with a dominant transport term. Finally, we will work on space-time formulations.

Appendix

In this appendix we report more details about the separation of variables strategy that we use to include in P_V some information on the geometry. A complete analysis of the geometry inclusion strategy will be addressed in a forthcoming work.

We incorporate in P_V some information on the parametrization present in the diagonal blocks A_{kk} by making approximations of the full matrix \mathfrak{C}_k (see equations (3.8), (3.10)), whose entries are functions of three variables that we denote with $c_{ij}^k(\boldsymbol{\eta})$:

$$\mathfrak{C}_k(\boldsymbol{\eta}) = \begin{bmatrix} c_{11}^k(\boldsymbol{\eta}) & c_{12}^k(\boldsymbol{\eta}) & c_{13}^k(\boldsymbol{\eta}) \\ c_{21}^k(\boldsymbol{\eta}) & c_{22}^k(\boldsymbol{\eta}) & c_{23}^k(\boldsymbol{\eta}) \\ c_{31}^k(\boldsymbol{\eta}) & c_{32}^k(\boldsymbol{\eta}) & c_{33}^k(\boldsymbol{\eta}) \end{bmatrix}.$$

We discard the off-diagonal terms and approximate the diagonal entries $c_{11}^k(\boldsymbol{\eta})$, $c_{22}^k(\boldsymbol{\eta})$ and $c_{33}^k(\boldsymbol{\eta})$ as follows (by the algorithm in [47, 48, 49])

$$\mathfrak{C}_k(\boldsymbol{\eta}) \approx \widehat{\mathfrak{C}}_k(\boldsymbol{\eta}) := \begin{bmatrix} \tau_1^k(\eta_1)\mu_2^k(\eta_2)\mu_3^k(\eta_3) & 0 & 0 \\ 0 & \mu_1^k(\eta_1)\tau_2^k(\eta_2)\mu_3^k(\eta_3) & 0 \\ 0 & 0 & \mu_1^k(\eta_1)\mu_2^k(\eta_2)\tau_3^k(\eta_3) \end{bmatrix}.$$

The approximation above is computed directly at the quadrature points, hence no function space has to be selected a-priori. The cost of this algorithm is proportional to the number of quadrature points, hence in our setting it requires $O(n_{el}p^d)$ FLOPs. This cost could be easily reduced by computing the approximation on a coarser grid of points, and then extending by interpolation. However this is not necessary, since such cost is already negligible in the context of the iterative procedures considered in this paper, as can be seen e.g. by comparing Tables 3 and 7.

Keeping the block-diagonal structure of P_V (cfr. (5.1)), we define for the TH discretization, $k = 1, 2, 3$ and $i, j = 1, \dots, n_{V,k}^{TH}$

$$\left[\widehat{P}_{V,k}^{TH} \right]_{i,j} := \int_{\widehat{\Omega}} \left(\nabla \widehat{B}_{\alpha,i}^{p+1} \right)^T \widehat{\mathfrak{C}}_k^{TH} \nabla \widehat{B}_{\alpha,j}^{p+1} d\boldsymbol{\eta},$$

while for the RT discretization, $k = 1, 2, 3$ and $i, j = 1, \dots, n_{V,k}^{RT}$

$$\begin{aligned} \left[\widehat{P}_{V,k}^{RT} \right]_{i,j} &:= \int_{\widehat{\Omega}} \left(\nabla \widehat{B}_{\alpha+\mathbf{e}_k,i}^{p+\mathbf{e}_k} \right)^T \widehat{\mathfrak{C}}_k^{RT} \nabla \widehat{B}_{\alpha+\mathbf{e}_k,j}^{p+\mathbf{e}_k} d\boldsymbol{\eta} + 2 \int_{\partial\widehat{\Omega}} \left[\frac{C_{pen}}{h} \widehat{B}_{\alpha+\mathbf{e}_k,i}^{p+\mathbf{e}_k} \mathbf{e}_k \cdot \left(\widehat{\mathfrak{C}}_k^{RT} \mathbf{e}_k \widehat{B}_{\alpha+\mathbf{e}_k,j}^{p+\mathbf{e}_k} \right) \right. \\ &\quad \left. - \left(\left(\nabla^s \left(\mathbf{e}_k \widehat{B}_{\alpha+\mathbf{e}_k,i}^{p+\mathbf{e}_k} \right) \hat{\mathbf{n}} \right) \cdot \left(\widehat{\mathfrak{C}}_k^{RT} \mathbf{e}_k \widehat{B}_{\alpha+\mathbf{e}_k,j}^{p+\mathbf{e}_k} \right) - \left(\left(\nabla^s \left(\mathbf{e}_k \widehat{B}_{\alpha+\mathbf{e}_k,j}^{p+\mathbf{e}_k} \right) \hat{\mathbf{n}} \right) \cdot \left(\widehat{\mathfrak{C}}_k^{RT} \mathbf{e}_k \widehat{B}_{\alpha+\mathbf{e}_k,i}^{p+\mathbf{e}_k} \right) \right) \right] d\widehat{\Gamma}. \end{aligned}$$

The preconditioners $\widehat{P}_{V,k}$ maintain the tensor structure of (5.4) and (5.5):

$$\begin{aligned} \widehat{P}_{V,1}^{TH} &= K_3^{1,TH} \otimes M_2^{1,TH} \otimes M_1^{1,TH} + M_3^{1,TH} \otimes K_2^{1,TH} \otimes M_1^{1,TH} + M_3^{1,TH} \otimes M_2^{1,TH} \otimes K_1^{1,TH}, \\ \widehat{P}_{V,2}^{TH} &= K_3^{2,TH} \otimes M_2^{2,TH} \otimes M_1^{2,TH} + M_3^{2,TH} \otimes K_2^{2,TH} \otimes M_1^{2,TH} + M_3^{2,TH} \otimes M_2^{2,TH} \otimes K_1^{2,TH}, \\ \widehat{P}_{V,3}^{TH} &= K_3^{3,TH} \otimes M_2^{3,TH} \otimes M_1^{3,TH} + M_3^{3,TH} \otimes K_2^{3,TH} \otimes M_1^{3,TH} + M_3^{3,TH} \otimes M_2^{3,TH} \otimes K_1^{3,TH}, \\ \widehat{P}_{V,1}^{RT} &= \widetilde{K}_3^{1,RT} \otimes \widetilde{M}_2^{1,RT} \otimes \widetilde{M}_1^{1,RT} + \widetilde{M}_3^{1,RT} \otimes \widetilde{K}_2^{1,RT} \otimes \widetilde{M}_1^{1,RT} + \widetilde{M}_3^{1,RT} \otimes \widetilde{M}_2^{1,RT} \otimes \widetilde{K}_1^{1,RT}, \\ \widehat{P}_{V,2}^{RT} &= \widetilde{K}_3^{2,RT} \otimes \widetilde{M}_2^{2,RT} \otimes \widetilde{M}_1^{2,RT} + \widetilde{M}_3^{2,RT} \otimes \widetilde{K}_2^{2,RT} \otimes \widetilde{M}_1^{2,RT} + \widetilde{M}_3^{2,RT} \otimes \widetilde{M}_2^{2,RT} \otimes \widetilde{K}_1^{2,RT}, \\ \widehat{P}_{V,3}^{RT} &= K_3^{3,RT} \otimes \widetilde{M}_2^{3,RT} \otimes \widetilde{M}_1^{3,RT} + M_3^{3,RT} \otimes \widetilde{K}_2^{3,RT} \otimes \widetilde{M}_1^{3,RT} + M_3^{3,RT} \otimes \widetilde{M}_2^{3,RT} \otimes \widetilde{K}_1^{3,RT}, \end{aligned}$$

where, for $d, k = 1, 2, 3$, the new pairs (K_k^d, M_k^d) and $(\widetilde{K}_k^d, \widetilde{M}_k^d)$ are

$$\begin{aligned} \left[K_k^{d,TH} \right]_{l,s} &= \int_{[0,1]} \tau_k^{d,TH}(\eta_k) (\hat{b}_{\alpha_k,l}^{p+1})'(\eta_k) (\hat{b}_{\alpha_k,s}^{p+1})'(\eta_k) d\eta_k, \\ \left[M_k^{d,TH} \right]_{l,s} &= \int_{[0,1]} \mu_k^{d,TH}(\eta_k) \hat{b}_{\alpha_k,l}^{p+1}(\eta_k) \hat{b}_{\alpha_k,s}^{p+1}(\eta_k) d\eta_k, \end{aligned}$$

for $l, s = 2, \dots, m_{\alpha_k}^{p+1} - 1$, and

$$\begin{aligned} \left[K_k^{d,RT} \right]_{l,s} &= \int_{[0,1]} \tau_k^{d,RT}(\eta_k) (\hat{b}_{\alpha_k+1,l}^{p+1})'(\eta_k) (\hat{b}_{\alpha_k+1,s}^{p+1})'(\eta_k) d\eta_k, \\ \left[M_k^{d,RT} \right]_{l,s} &= \int_{[0,1]} \mu_k^{d,RT}(\eta_k) \hat{b}_{\alpha_k+1,l}^{p+1}(\eta_k) \hat{b}_{\alpha_k+1,s}^{p+1}(\eta_k) d\eta_k, \end{aligned}$$

for $l, s = 2, \dots, m_{\alpha_k+1}^{p+1} - 1$, and finally

$$\begin{aligned} \left[\widetilde{K}_k^{d,RT} \right]_{l,s} &= \int_{[0,1]} \tau_k^{d,RT}(\eta_k) (\hat{b}_{\alpha_k,l}^p)'(\eta_k) (\hat{b}_{\alpha_k,s}^p)'(\eta_k) d\eta_k - \left[\tau_k^{d,RT}(1) (\hat{b}_{\alpha_k,l}^p)'(1) \hat{b}_{\alpha_k,s}^p(1) \right. \\ &\quad - \tau_k^{d,RT}(0) (\hat{b}_{\alpha_k,l}^p)'(0) \hat{b}_{\alpha_k,s}^p(0) + \tau_k^{d,RT}(1) (\hat{b}_{\alpha_k,s}^p)'(1) \hat{b}_{\alpha_k,l}^p(1) \\ &\quad - \tau_k^{d,RT}(0) (\hat{b}_{\alpha_k,s}^p)'(0) \hat{b}_{\alpha_k,l}^p(0) - 2 \frac{C_{pen}}{h} (\tau_k^{d,RT}(1) \hat{b}_{\alpha_k,l}^p(1) \hat{b}_{\alpha_k,s}^p(1) \\ &\quad \left. + \tau_k^{d,RT}(0) \hat{b}_{\alpha_k,l}^p(0) \hat{b}_{\alpha_k,s}^p(0)) \right], \\ \left[\widetilde{M}_k^{d,RT} \right]_{l,s} &= \int_{[0,1]} \mu_k^{d,RT}(\eta_k) \hat{b}_{\alpha_k,l}^p(\eta_k) \hat{b}_{\alpha_k,s}^p(\eta_k) d\eta_k, \end{aligned}$$

for $l, s = 1, \dots, m_{\alpha_k}^p$.

Acknowledgments

The authors were partially supported by the European Research Council through the FP7 Ideas Consolidator Grant *HIGEOM* n.616563. The authors are members of the Gruppo Nazionale Calcolo Scientifico-Istituto Nazionale di Alta Matematica (GNCS-INDAM), and the third author was partially supported by GNCS-INDAM for this research. This support are gratefully acknowledged.

References

- [1] T. J. R. Hughes, J. A. Cottrell, Y. Bazilevs, Isogeometric analysis: CAD, finite elements, NURBS, exact geometry and mesh refinement, *Computer Methods in Applied Mechanics and Engineering* 194 (39) (2005) 4135–4195.
- [2] J. A. Cottrell, T. J. R. Hughes, Y. Bazilevs, *Isogeometric analysis: toward integration of CAD and FEA*, John Wiley & Sons, 2009.
- [3] L. Beirão da Veiga, A. Buffa, G. Sangalli, R. Vázquez, Mathematical analysis of variational isogeometric methods, *Acta Numerica* 23 (2014) 157–287.
- [4] J. A. Evans, Y. Bazilevs, I. Babuška, T. J. R. Hughes, n -widths, sup-infs, and optimality ratios for the k -version of the isogeometric finite element method, *Comput. Methods Appl. Mech. Engrg.* 198 (2009) 1726–1741.
- [5] T. J. R. Hughes, A. Reali, G. Sangalli, Duality and unified analysis of discrete approximations in structural dynamics and wave propagation: comparison of p -method finite elements with k -method NURBS, *Comput. Methods Appl. Mech. Engrg.* 197 (49-50) (2008) 4104–4124.
- [6] H. Gómez, V. Calo, Y. Bazilevs, T. J. R. Hughes, Isogeometric analysis of the Cahn-Hilliard phase field model, *Comput. Methods Appl. Mech. Engrg.* 49–50 (2008) 4333 – 4352.
- [7] A. Buffa, J. Rivas, G. Sangalli, R. Vázquez, Isogeometric discrete differential forms in three dimensions, *SIAM Journal on Numerical Analysis* 49 (2) (2011) 818–844.

- [8] Y. Bazilevs, L. Beirao da Veiga, J. A. Cottrell, T. J. R. Hughes, G. Sangalli, Isogeometric analysis: approximation, stability and error estimates for h-refined meshes, *Math. Mod. and Meth. Appl. Sc.* 16 (07) (2006) 1031–1090.
- [9] A. Buffa, C. De Falco, G. Sangalli, Isogeometric analysis: stable elements for the 2d Stokes equation, *International Journal for Numerical Methods in Fluids* 65 (11-12) (2011) 1407–1422.
- [10] A. Bressan, Isogeometric regular discretization for the Stokes problem, *IMA journal of numerical analysis* 31 (4) (2010) 1334–1356.
- [11] A. Bressan, G. Sangalli, Isogeometric discretizations of the Stokes problem: stability analysis by the macroelement technique, *IMA Journal of Numerical Analysis* 33 (2) (2012) 629–651.
- [12] J. A. Evans, T. J. R. Hughes, Isogeometric divergence-conforming B-splines for the Darcy–Stokes–Brinkman equations, *Mathematical Models and Methods in Applied Sciences* 23 (04) (2013) 671–741.
- [13] J. A. Evans, T. J. R. Hughes, Isogeometric divergence-conforming B-splines for the steady Navier–Stokes equations, *Mathematical Models and Methods in Applied Sciences* 23 (08) (2013) 1421–1478.
- [14] J. A. Evans, T. J. R. Hughes, Isogeometric divergence-conforming B-splines for the unsteady Navier–Stokes equations, *Journal of Computational Physics* 241 (2013) 141–167.
- [15] N. Collier, D. Pardo, L. Dalcin, M. Paszynski, V. M. Calo, The cost of continuity: a study of the performance of isogeometric finite elements using direct solvers, *Computer Methods in Applied Mechanics and Engineering* 213 (2012) 353–361.
- [16] A. Buffa, H. Harbrecht, A. Kuno, G. Sangalli, BPX-preconditioning for isogeometric analysis, *Computer Methods in Applied Mechanics and Engineering* 265 (2013) 63–70.
- [17] L. Beirão da Veiga, D. Cho, L. F. Pavarino, S. Scacchi, BDDC preconditioners for isogeometric analysis, *Mathematical Models and Methods in Applied Sciences* 23 (06) (2013) 1099–1142.
- [18] M. Donatelli, C. Garoni, C. Manni, S. Serra-Capizzano, H. Speleers, Robust and optimal multi-iterative techniques for IgA Galerkin linear systems, *Computer Methods in Applied Mechanics and Engineering* 284 (2015) 230–264.
- [19] C. Hofreither, S. Takacs, Robust multigrid for isogeometric analysis based on stable splittings of spline spaces, *SIAM Journal on Numerical Analysis* 55 (4) (2017) 2004–2024.
- [20] G. Sangalli, M. Tani, Isogeometric preconditioners based on fast solvers for the Sylvester equation, *SIAM Journal on Scientific Computing* 38 (6) (2016) A3644–A3671.
- [21] A. M. Côrtes, A. L. G. A. Coutinho, L. Dalcin, V. M. Calo, Performance evaluation of block-diagonal preconditioners for the divergence-conforming B-spline discretization of the Stokes system, *Journal of Computational Science* 11 (2015) 123–136.
- [22] A. M. Côrtes, L. Dalcin, A. F. Sarmiento, N. Collier, V. M. Calo, A scalable block-preconditioning strategy for divergence-conforming B-spline discretizations of the Stokes problem, *Computer Methods in Applied Mechanics and Engineering* 316 (2017) 839–858.

- [23] L. Pavarino, S. Scacchi, Isogeometric block FETI-DP preconditioners for the Stokes and mixed linear elasticity systems, *Computer Methods in Applied Mechanics and Engineering* 310 (2016) 694–710.
- [24] C. Coley, J. Benzaken, J. A. Evans, A geometric multigrid method for isogeometric compatible discretizations of the generalized Stokes and Oseen problems, arXiv preprint arXiv:1705.09282.
- [25] S. Takacs, Robust multigrid methods for isogeometric discretizations of the Stokes equations, arXiv preprint arXiv:1705.04481.
- [26] H. C. Elman, D. J. Silvester, A. J. Wathen, *Finite elements and fast iterative solvers: with applications in incompressible fluid dynamics*, Numerical Mathematics & Scientific Computation, 2014.
- [27] V. Simoncini, Computational methods for linear matrix equations, *SIAM Review* 58 (3) (2016) 377–441.
- [28] M. O. Deville, P. F. Fischer, E. H. Mund, *High-order methods for incompressible fluid flow*, Cambridge University Press, 2002.
- [29] R. E. Lynch, J. R. Rice, D. H. Thomas, Direct solution of partial difference equations by tensor product methods, *Numerische Mathematik* 6 (1) (1964) 185–199.
- [30] G. Sangalli, M. Tani, Matrix-free isogeometric analysis: the computationally efficient k -method, arXiv preprint arXiv:1712.08565.
- [31] C. De Boor, *A practical guide to splines; rev. ed.*, Applied Mathematical Sciences, Springer, Berlin, 2001.
- [32] T. G. Kolda, B. W. Bader, Tensor decompositions and applications, *SIAM review* 51 (3) (2009) 455–500.
- [33] M. Benzi, G. H. Golub, J. Liesen, Numerical solution of saddle point problems, *Acta numerica* 14 (2005) 1–137.
- [34] A. Wathen, D. Silvester, Fast iterative solution of stabilised Stokes systems. Part I: Using simple diagonal preconditioners, *SIAM Journal on Numerical Analysis* 30 (3) (1993) 630–649.
- [35] D. Silvester, A. Wathen, Fast iterative solution of stabilised Stokes systems Part II: Using general block preconditioners, *SIAM Journal on Numerical Analysis* 31 (5) (1994) 1352–1367.
- [36] M. F. Murphy, G. H. Golub, A. J. Wathen, A note on preconditioning for indefinite linear systems, *SIAM J. Sci. Comput.* 21 (6) (2000) 1969–1972.
- [37] C. C. Paige, M. A. Saunders, Solution of sparse indefinite systems of linear equations, *SIAM journal on numerical analysis* 12 (4) (1975) 617–629.
- [38] C. Keller, N. I. M. Gould, A. J. Wathen, Constraint preconditioning for indefinite linear systems, *SIAM J. Matrix Anal. Appl.* 21 (4) (2000) 1300–1317.
- [39] Y. Saad, M. H. Schultz, GMRES: A generalized minimal residual algorithm for solving nonsymmetric linear systems, *SIAM Journal on scientific and statistical computing* 7 (3) (1986) 856–869.
- [40] P. P. Grinevich, M. A. Olshanskii, An iterative method for the stokes-type problem with variable viscosity, *SIAM Journal on Scientific Computing* 31 (5) (2009) 3959–3978.

- [41] P. G. Ciarlet, *Mathematical elasticity. Vol. I*, Vol. 20 of *Studies in Mathematics and its Applications*, North-Holland Publishing Co., Amsterdam, 1988, three-dimensional elasticity.
- [42] J. A. Evans, T. J. R. Hughes, Explicit trace inequalities for isogeometric analysis and parametric hexahedral finite elements, *Numerische Mathematik* 123 (2) (2013) 259–290.
- [43] R. Vázquez, A new design for the implementation of isogeometric analysis in Octave and Matlab: *GeoPDEs 3.0*, *Computers & Mathematics with Applications* 72 (3) (2016) 523–554.
- [44] L. Sorber, M. Van Barel, L. De Lathauwer, *Tensorlab v2. 0*, Available online, URL: www.tensorlab.net.
- [45] F. Calabrò, G. Sangalli, M. Tani, Fast formation of isogeometric galerkin matrices by weighted quadrature, *Computer Methods in Applied Mechanics and Engineering* 316 (2017) 606–622.
- [46] A. Mantzaflaris, B. Jüttler, B. N. Khoromskij, U. Langer, Low rank tensor methods in Galerkin-based isogeometric analysis, *Comput. Methods Appl. Mech. Engrg.* 316 (2017) 1062–1085.
- [47] S. Diliberto, E. Straus, On the approximation of a function of several variables by the sum of functions of fewer variables, *Pacific Journal of Mathematics* 1 (2) (1951) 195–210.
- [48] E. L. Wachspress, *Generalized ADI preconditioning*, *Computers & mathematics with applications* 10 (6) (1984) 457–461.
- [49] E. L. Wachspress, *The ADI model problem*, Springer, 2013.